(19) DANMARK

(10) **DK/EP 3443610 T3**

Patent- og Varemærkestyrelsen

(12) Oversættelse af europæisk patentskrift

(51) Int.Cl.: ***H 01 M 8/04298 (2016.01)*** ***H 01 M 8/04537 (2016.01)*** ***H 01 M 8/04664 (2016.01)***

(45) Oversættelsen bekendtgjort den: **2022-02-14**

(80) Dato for Den Europæiske Patentmyndigheds bekendtgørelse om meddelelse af patentet: **2021-12-15**

(86) Europæisk ansøgning nr.: **17725502.3**

(86) Europæisk indleveringsdag: **2017-04-11**

(87) Den europæiske ansøgnings publiceringsdag: **2019-02-20**

(86) International ansøgning nr.: **DE2017100295**

(87) Internationalt publikationsnr.: **WO2017178016**

(30) Prioritet: **2016-04-12 DE 102016106735**

(84) Designerede stater: **AL AT BE BG CH CY CZ DE DK EE ES FI FR GB GR HR HU IE IS IT LI LT LU LV MC MK MT NL NO PL PT RO RS SE SI SK SM TR**

(73) Patenthaver: **Zentrum für Sonnenenergie- und Wasserstoff-Forschung Baden-Württemberg Gemeinnützige Stiftung, Meitnerstrasse 1, 70563 Stuttgart, Tyskland**
thyssenkrupp Marine Systems GmbH, Werftstraße 112-114, 24143 Kiel, Tyskland

(72) Opfinder: **DAO, Tuan Ahn, Einsingerstr. 24, 89073 Ulm, Tyskland**
Dannenberg, Norbert, Kählstorfer Weg 11, 23628 Krummesse, Tyskland
ENZ, Simon, Haydnstraße 3, 72535 Heroldstadt, Tyskland
KLAGES, Merle, Eberhardstraße 41, 89073 Ulm, Tyskland
Pommer, Hans, Dorfstraße 16, 24360 Barkelsby, Tyskland
SCHOLTA, Joachim, Hirschstraße 35, 89278 Niersingen, Tyskland

(74) Fuldmægtig i Danmark: **COPA COPENHAGEN PATENTS K/S, Rosenørns Allé 1, 2. sal, 1970 Frederiksberg C, Danmark**

(54) Benævnelse: **PROGNOSEMODEL FOR EN BRÆNDSTOFCELLE BASERET PÅ ET TILSVARENDE KREDSLØBSDIAGRAM**

(56) Fremdragne publikationer:
EP-A1- 2 551 688
EP-A1- 2 845 255
EP-A2- 1 501 146
EP-A2- 1 646 101
DE-A1- 10 036 572
DE-A1- 10 220 172
US-A1- 2003 204 328
US-A1- 2016 006 061
LEE J H ET AL: "Development of a method to estimate the lifespan of proton exchange membrane fuel cell using electrochemical impedance spectroscopy", JOURNAL OF POWER SOURCES, ELSEVIER SA, CH, Bd.

Fortsættes ...

195, Nr. 18, 15. September 2010 (2010-09-15), Seiten 6001-6007, XP027148134, ISSN: 0378-7753 [gefunden am 2010-07-16]
Vadim F. Lvovich: "Multiple-sine impedance equipment" In: "Impedance Spectroscopy", 2. Juli 2012 (2012-07-02), John Wiley & Sons, Inc., Hoboken, New Jersey, XP055394522, ISBN: 978-0-470-62778-5 Seiten 169-170, das ganze Dokument

Fuel Cell Forecast Model Based on an Equivalent Circuit Diagram

The invention relates to a method for diagnosing fuel cells and forecasting a service life expectancy or predicting a residual life of fuel cells. In addition, it relates to a device for diagnosis and prognosis of fuel cells.

The current trend towards renewable energies, in particular in drive systems for the automotive industry, has led to fuel cell technology being further developed, so that it can now be used not only in stationary operation, but also in the mobile sector, whereby the use not only in the automotive industry, but, due to the progressive miniaturization also in portable devices, such as portable power generators or mobile phones, is possible.

The further development of fuel cells requires comprehensive and detailed monitoring of the components of a fuel cell. Due to the complex electrochemical processes within a fuel cell, previous methods for diagnosing the state of fuel cells or of their components and/or statements regarding the service life prediction of the fuel cell or of its components are still insufficient.

For the previously known methods for diagnosing and forecasting the service life of fuel cells up to now, current/voltage characteristics have been modeled which allow an acceptable forecast of the service life, however cannot give precise information as to which of the fuel cell components or fuel cell parameters are changing to what extent. In particular, it is difficult to distinguish between resistive effects, incipient mass transfer effects as well as catalytic effects in the current/voltage characteristic modeling for diagnosing or forecasting the service life. One method of diagnosis is impedance spectroscopy, wherein a comparison between reference values and a currently measured impedance value allows for a diagnosis. However, a possible extrapolation to the useful remaining life is subject to many uncertainties and signal noise, entailing considerable uncertainty regarding the indication of the remaining service life of the fuel cell or individual fuel cell components thereof.

It is therefore an object of the invention to provide a method and a device for diagnosing fuel cells, and, in particular, a method and a device which allow for a more accurate

prediction of the service life or the remaining service life of the fuel cell or of parts thereof.

LEE J H ET AL: "Development of a method to estimate the lifespan of proton exchange membrane fuel cell using electrochemical impedance spectroscopy" JOURNAL OF POWER SOURCES, ELSEVIER SA, CH, Bd. 195, Nr. 18 describes a lifespan analysis of a fuel cell wherein the degradation of the cathode is being analyzed.

DE 100 36 572 A1 (BOSCH GMBH ROBERT [DE]) 14 February 2002 (2002-02-14) describes a fuel cell system with a fuel cell unit and a fuel supply unit, wherein there is provided a measuring unit for measuring at least one first operating parameter of the fuel cell unit, which enables nearly complete monitoring of the inner operating mode of the fuel cell unit, wherein the number of sensors applied, and thereby the complexity of the system, is being reduced. This is achieved by providing an evaluation unit for evaluating a temporal change in the first operating parameter of the fuel cell unit in dependence of a known, temporal change of at least a second operating parameter of the fuel cell system.

The object of the invention is achieved by the features of the independent claims.

The invention is based on the basic idea to determine the impedances with an excitation signal, for example comprising at least two different excitation frequencies, as a function of excitation frequencies at fixed time intervals and to determine the best fitting equivalent circuit diagram values or parameters by means of a data regression method. Based thereon, the parameters of the equivalent circuit diagram component may be determined at different times. These parameters may already be used for a diagnosis of the components of the fuel cell. Based on the thus determined parameters for the equivalent circuit diagram components for different times, a time dependence of the parameters of the equivalent circuit diagram components is determined.

Based on this time dependence for the parameters of the individual equivalent circuit diagram components, a forecast regarding the components is possible.

That is, for the measurement results of the impedance spectroscopy in the form of impedances $Z_n(f, t)$, a function Y(f) is determined, which can be parameterized, wherein corresponding elements or subassemblies of the fuel cell are assigned to the parameterizable equivalent circuit diagram components of the equivalent circuit diagram.

The measurement results $Z_n(f, t)$ have a real and an imaginary part and, plotted against each other as a graphic function, form a more or less semicircular profile of the function. This profile changes during the measurements at different times. To the impedances determined at a time by the impedance spectroscopy, a function Y(f) is assigned or fitted by data regression, which can be composed of partial functions $Y_1 + Y_2 + Y_3 + Y_4$ or functional components. Each functional component or partial function of the equivalent circuit diagram corresponds to an element or a subassembly of the fuel cell. Based on this composite function, it is then possible to determine the parameters of the equivalent circuit diagram components that are characteristic of the fitted function profile. That is, real values are obtained for the individual equivalent circuit diagram components or parameters of a functional component.

Thus, at fixed operating points of the measurement, a time-dependent profile for the parameters of the fuel cell and thus a change in the parameters may be determined by repeatedly applying the at least two excitation frequencies, so that a degradation of individual functional components of the fuel cell may be inferred.

Therefore, a very accurate mapping of degradation phenomena to functional components of a fuel cell is possible.

According to one aspect of the invention, a method for diagnosing and/or forecasting the service life of a fuel cell is provided, comprising the steps of applying an excitation signal f_n to the fuel cell at a first time t_1, detecting impedances at the frequencies of the excitation signal f_n at the first time t_1, determining a function Y(f) for the detected impedances Z_n (f_n, t_1) containing functional components of a predetermined equivalent circuit diagram of the fuel cell, each functional component including at least one equivalent circuit diagram component, the values of which can be parameterized, determining at least one parameter of at least one equivalent circuit diagram component

of at least one functional component based on the determined function Y(F) matching the impedances $Z_n(f_n, t_1)$ detected at the first time t_1; applying the excitation signal f_n to the fuel cell at a second time t_2, detecting impedances $Z_n(f_n, t_2)$ at the frequencies of the excitation signal f_n at at least one second time t_2, determining the at least one parameter of the at least one equivalent circuit diagram component of the at least one functional component based on the determined function Y(f) matching the impedances $Z_n(f_n, t_2)$ detected at the second time t_2; determining at least one time dependence for the at least one parameter based on the parameters determined for the first and second times t_1, t_2; detecting at least one sign of degradation based on the time dependence of the at least one parameter for at least one functional component of the equivalent circuit diagram of the fuel cell.

Preferably, signs of degradation are detected based on the change of the impedances Z_n (f_n, t_2) at time t_2 in comparison to the impedances Z_n (f_n, t_1) at time t_1.

Preferably, a functional component of the function is represented by at least one equivalent circuit diagram component or an interconnection of a plurality of them. Each functional component represents a component, element or subassembly of the fuel cell.

Preferably, to determine signs of degradation of individual functional components, at least one threshold value overshooting and/or threshold value undershooting of at least one parameter of at least one equivalent circuit diagram component is calculated based on its time dependence. The advantage of this approach is that, in addition to the mere degradation of the fuel cell being detectable from the current-voltage behavior, also the affected functional component of the fuel cell may be recognized. For example, it is possible to thus distinguish between a membrane resistance related degradation and a cathode catalyst related degradation.

According to the invention, a slope of the at least one time dependence of an equivalent circuit diagram component is determined in order to determine signs of degradation. The advantage of this procedure is that, in addition to the mere degradation of the fuel cell being detectable from the current-voltage behavior, a degradation of the component of the fuel cell related to the functional component can also be recognized. For example, it

is possible to thus distinguish between a membrane resistance related degradation and a cathodic-catalyst related degradation.

In order to determine the function Y(f) based on the detected impedances Z_n (f_n, t), the detected impedances $Z_n(f_n, t)$ can be grouped. For this, a functional component Y_1, Y_2, Y_3 or Y_4 with at least one characteristic equivalent circuit diagram component R_1-R_4 and C_1-C_4 may be assigned to each group of impedances $Z_n(f_n, t)$.

The impedances $Z_n(f_n, t)$ detected at high frequencies which are represented on the left side of the semicircle in the Nyquist plot, are characteristic for the membrane resistance and are represented by the functional component Y_2 in the function Y(f) and in the equivalent circuit diagram. The impedances Z_n (f_n, t) detected at frequencies of, e. g., 1 to 50 Hz are characteristic for the cathode and are represented by the functional component Y_1 in the function Y(f) and in the equivalent circuit diagram. The impedances Z_n (f_n, t) detected at frequencies of, e. g., 100 to 1000 Hz are characteristic for the anode and are represented by the functional component Y_3 in the function Y(f) and in the equivalent circuit diagram. The impedances $Z_n(f_n, t)$ detected at low frequencies are characteristic for the mass transfer and are represented by the functional component Y_4 in the function Y(F) and in the equivalent circuit diagram. The ranges of the functional components Y_1, Y_3 and Y_4 overlap.

Preferably, at least one parameter for a functional component of the function Y(f) is determined based on the detected impedances $Z_n(f_n, t)$ at the first time t1 and/or second time t2. Here, a particularly characteristic parameter can be determined which is particularly meaningful with respect to the degradation, e. g., the cell resistance. Simple parameters determinable directly could be determined, for example in the range between 500 Hz and 5000 Hz, which can be correlated directly with the membrane resistance, since all other functional components with capacitances are short-circuited by the capacitances and are not negligible. That is, the higher the frequencies of the excitation signal, the clearer is the influence of the membrane resistance at the detected impedances.

Preferably, however, a parameterizable function Y(f) is assigned to the detected impedances $Z_n(f_n, t)$ by means of data regression. Here, for example, the method of least squares can be applied.

In particular, at least one parameter of the function Y(f) can be set to a predetermined value or a predetermined value range with upper and/or lower limit. For this purpose, empirical values may be used. This reduces the complexity of the parameter determination. The parameters whose time evolution is not critical for forecasting the service life, may be provided with fixed values or upper and/or lower limits. By means of these limitations and/or definitions, further unambiguous assignments of the individual equivalent circuit diagram components to components/subassemblies of the fuel cell may be made possible.

In order to make a forecast of the service life, a threshold value undershooting or overshooting of a parameter of at least one equivalent circuit diagram component may be monitored based on the determined time dependence. That is, when a value of a parameter exceeds or falls below a predefined value at a certain time, it is possible to infer a special aging stage or imminent total failure. The advantage of this approach is that, via the assignment of the equivalent circuit diagram component and the functional component to the component/subassembly of the fuel cell, an identification of the life-limiting component/subassembly may thus be performed.

Preferably, based on the determined time dependence of an equivalent circuit diagram component, a failure time t_x of the fuel cell in case of an overshooting and/or an undershooting of a predetermined resistance value or capacitance value of an equivalent circuit diagram component is determined. However, the method according to the invention can also determine whether the fuel cell will still be functional at time x. This indication is particularly important when using fuel cells for the autonomous operation of systems.

Preferably, the function Y(f) of the equivalent circuit diagram is being determined for at least a first current density (i_1) and a second current density (i_2). On the basis of the determination of the parameters and, therefrom, of the function Y(f, i) for different

current densities, the aging process may be determined as a function of the current density (i). That is, even for different load scenarios, e. g., at different current densities, a forecast of service life is possible.

In the method according to the invention, the measurements for determining the impedances at defined operating points (T, humidity, degree of conversion) are performed.

In addition to the detection of the impedances $Z_n(f)$ at the different times t1, t2, associated current/voltage characteristics of the fuel cell may be detected. From this, voltage values may then be predicted according to a method given below, and the accuracy of the determined function Y(f, i, t) may be evaluated by comparison with the measured voltage values.

Preferably, different excitation frequencies f_n may be used as the excitation signal f_n. In a preferred embodiment, when different current amplitudes are used as excitation frequencies f_n, the impedances are determined from voltage amplitudes. When different voltage amplitudes are used as excitation frequencies, the impedances are determined from current amplitudes.

Preferably, in the case of a fuel cell which comprises a plurality of individual cells connected in series, the impedances of all individual cells of the fuel cell may also be detected with only one current excitation over the entire cell stack. That is, with the method according to the invention, a forecast of the individual cells in terms of their service life and their component behavior is also possible.

Preferably, half wave amplitudes of the excitation frequencies are less than 10 mAs/cm^2 with respect to the active area of a single cell, and a voltage amplitude is less than 10 mV with respect to a single cell so as not to stress the fuel cell. The choice of such an amplitude according to the invention allows a high signal-to-noise ratio in typical fuel cells with respect to, e. g., the voltage response to the current excitation signal by selecting an amplitude which is not unnecessarily small, while, on the other hand, the

amplitude is still sufficiently small to avoid inadvertent temporary generation of gas deficiency conditions in a typical fuel cell.

Alternatively, half-wave amplitudes of the excitation frequencies may be less than 10 mAs/cm^2 with respect to the active area of a single cell so as not to stress the fuel cell, and a voltage amplitude may be greater than 10 mV with respect to a single cell in order to be able to evaluate resulting harmonic components.

Preferably, the excitation signal f_n may at least be formed from: a combination of at least two sinusoidal signals, a combination of at least two base frequencies with non-sinusoidal signal profile, or a combination of at least one sinusoidal and at least one non-sinusoidal signal.

Preferably, the excitation frequencies may be a suitable multiple of each other and/or may be added opposite in phase in order to keep the excitation amplitude as low as possible at high single frequency amplitude. The advantage of this method is that, with a favorable signal-to-noise ratio, the smallest possible charge amplitude is generated and thus the fuel cell is stressed only minimally.

In particular, a time of a voltage undershooting for the fuel cell may be determined with the determined function Y(f, t) and the measured current/voltage characteristics.

In particular, a time of a voltage undershooting may be determined with the determined function Y (f, t, i) and a measured or modeled no-load voltage and the current/voltage characteristics calculated therefrom.

The object is also achieved with a device for diagnosing and/or forecasting the service life of a fuel cell, comprising: a frequency generator for generating and applying at least one excitation signal f_n to the fuel cell at at least first and second times t_1, t_2; a measuring unit for detecting impedances $Z_n(f_n, t_1)$ and $Z_n(f_n, t_2)$ at the excitation frequencies of the excitation signal f_n at the at least first and second times t_1, t_2; a data regression module for determining a function Y(f) for impedances Z_n (f_n, t_1) detected at a first time t_1, wherein the function Y(f) contains functional components of an equivalent circuit diagram of a

fuel cell, wherein each functional component contains at least one equivalent circuit diagram component, the values of which can be parameterized, and for determining at least one parameter of the at least one equivalent circuit diagram component of the at least one functional component based on the determined function Y(f) matching the impedances Z_n (f_n, t_1) and Z_n (f_n, t_2) detected at the first and second times t_1, t_2; an evaluation unit for determining a time dependence for the at least one parameter of the equivalent circuit diagram based on the parameters determined for the first and second times t1, t2 and for detecting at least one sign of degradation of a component of the fuel cell based on the time dependence of the at least one parameter of the equivalent circuit diagram for the at least one functional component of the fuel cell, wherein, in order to determine the at least one sign of degradation, an increase in the time dependence of an equivalent circuit component is being determined.

In a preferred embodiment, the detection of the impedances $Z_n(f_n, t_1)$ and $Z_n(f_n, t_2)$ takes place in a component, module or unit of the device, wherein the data analysis (FFT, Z(f) determination) and equivalent circuit diagram parameterization may take place in a second component or unit. The regression of the equivalent circuit diagram parameters over time and the evaluation of this functionality may be done separately in another component or unit. However, some or all of the components or units may be grouped together or further subcomponents may be used in the device.

The sign of degradation may be output in a general form, i. e., for example as a tendency, or in a specified form, for example as a concrete time indication, e. g. by means of a monitor, digital information, a signal lamp or a message among other methods.

Preferably, measurement series are carried out for at least two different current densities i in order to therefrom determine a functional relationship between the parameters for different load scenarios of the fuel cell.

In addition, a voltage function may be derived which may be used to detect an undershooting of a predetermined limit value for the fuel cell voltage and to issue a corresponding alarm. In particular, the time prediction of the fuel cell voltage is of considerable importance in practice for forecasting the service life.

In addition, a comparison of different voltage values over time by means of extrapolation may be used to determine a time forecast for the fuel cell voltage falling below a limit value and thus to predict when a failure of corresponding components/subassemblies of a fuel cell or the entire fuel cell can be expected.

Compared to the prior art in which the impedance spectroscopy is used for diagnosis, this results in a possibility to make a forecast of the service life with much higher accuracy, because mapping one or more degradation effects to individual components or individual parts or subassemblies of the fuel cell is possible and the proposed regression and extrapolation method additionally allows for a more accurate forecast of residual service life.

By considering at least two different current densities, it is possible to detect mass transfer limitations of the fuel cell by degradation of, for example, the gas diffusion layer.

For this purpose, a parameterized function which may either be a permanently parameterized function or may be combined with a look-up table is stored for at least one equivalent circuit diagram. In addition to fixedly parameterized equivalent circuit diagram components, the function may also contain adjustable parameters.

According to the invention, considering the obtained equivalent circuit diagram parameters as a regression function, e. g.as a linear function of time, allows a lower variance of the predicted values compared to other methods and compared to other model approaches. Furthermore, this approach allows recognition of "outbreaks" of parameters from the expected evolution and thus both an on-demand adjustment of the forecast and a recognition of special events influencing the degradation of the fuel cell.

The generation of the equivalent circuit diagram by means of discrete individual components allows for assigning the functional components to physicochemical processes, e. g. the anode and cathode polarization as well as the mass transfer and membrane resistance. The definition or limitation of certain parameters used in the determination of the equivalent circuit diagram parameters allows for a stable assignment

of equivalent circuit diagram components to specific processes and furthermore causes reduction or suppression of underdetermined states of the system and thus a low-correlation behavior of the equivalent circuit diagram parameters.

Monitoring equivalent circuit parameters for compliance with limits allows for an immediate indication of the ongoing degradation of certain components, e. g. the membrane when a maximum value of the membrane resistance is exceeded.

The measurement of the current-voltage behavior of the cell taking place in parallel with the determinations of Z_n (f, i, t) permits a comparison between the cell voltages calculated from the no-load voltage and the impedances Z (i, t).

On the one hand, the cell voltage U (i, t) may be determined from

$$U(i,t) = U_0 - \int_{i=0}^{i} Z(i,t)di$$

and, on the other hand, it is known from the measured U_n (i, t) at the respective time t. From the deviations between the measured U_n(i, t) and the calculated U(i, t), the accuracy of the calculated Z(i, t) may be inferred and this information may be used to select the best suited method for determining Z(i, t).

The determination of the impedances Z_n(f) from current amplitudes is preferred over the determination of the impedances Z_n(f, i, t) from voltage amplitudes, which is also possible, since, in this way, a simultaneous determination of Z_n(f, i, t) without mutual interference for both the stack and the single cell voltages of a stack of multiple fuel cells is possible.

The limitation of the excitation amplitudes to values of 5 to 20 mAs/cm^2, particularly preferably below 10 mAs/cm^2, according to the invention, avoids additional stress for the fuel cell due to undersupply conditions with at least one reactant which could otherwise possibly occur and which could lead to, under some circumstances considerable, additional degradation.

Interleaving the excitation frequencies according to the invention such that the excitation frequencies are a suitable multiple of each other and/or are added opposite in phase allows to keep the excitation amplitude as low as possible at high single frequency amplitude and thus to obtain a high signal-to-noise ratio for the measurement while obtaining the lowest possible charge amplitude per half-wave of the fundamental frequency, which minimizes the risk of temporary undersupply conditions.

The invention will be described in more detail below with reference to the figures. In the figures:

Fig. 1 shows a schematic structure of a fuel cell;
Figs. 2a, 2b show an exemplary excitation frequency and the response based thereon;
Fig. 3a shows an exemplary equivalent circuit diagram with functional components;
Fig. 3b shows a representation of the grouping of impedances in the Nyquist plot and their mapping to functional components;
Fig. 4a shows impedances at different times at a first current density;
Fig. 4b shows impedances at different times at a second current density;
Fig. 4c shows impedances at different times at a third current density;
Figs. 5a-5d show a representation of the parameters of the equivalent circuit diagram after different times at different current densities;
Figs. 6a-6c show the time dependence of the parameters of the equivalent circuit diagram at different current densities;
Fig. 7 shows a flow diagram for illustrating the method according to the invention;
Fig. 8 is a schematic representation of a device according to the invention.

Fig. 1 shows a schematic structure of a fuel cell. Fuel cells are galvanic elements in which the chemical energy is converted directly into electrical energy, wherein the respective oxidation and reduction processes occur spatially separated from each other in so-called half-cells. As a result, the electrons released during the oxidation may be conducted to, for example, an electric motor via an outer conductor circuit in which a load is incorporated and thus electrical work may be performed. In contrast to batteries, the reactants hydrogen and oxygen are supplied continuously in fuel cells, so that power generation without charge times is enabled. The direct energy conversion from chemical

to electrical energy results in greater efficiency compared to conventional internal combustion engines.

In addition, no mechanical components are moved, whereby a low-noise operation without mechanical wear is possible. Fuel cells operate in a similar manner to batteries, but have the advantage over battery-operated devices, for example in vehicles, that long charging times are not necessary and refueling with the reactances similar to internal combustion engines is possible.

An example of the fuel cells only mentioned herein for illustrating purposes is the polymer electrolyte membrane fuel cell (PEMFC). It is one of the low-temperature fuel cells, whereby a distinction is made between low-temperature (LT) PEMFC with operating temperature less than or equal to 90 °C and high-temperature (HT) PEMFC with operating temperatures greater than 100 °C.

For low-temperature fuel cells, typically a proton-conducting membrane, for example made of perfluorinated sulfonic acid polymer, is used, wherein for HT-PEMFC a membrane of polybenzimidazole (PBI) which is mixed with phosphoric acid as electrolyte is used. In both cases, the oxonium (H_30^+) ion is transported across the membrane as a charge carrier. As the fuel gas, pure hydrogen or reformate gas is used on the anode side, and, as the oxidizing agent, air or even pure oxygen is used on the cathode side. The underlying cell reactions in a PEMFC are as follows:

Anode: $H_2 + 2\ H_2O \Leftrightarrow H_3O^+ + 2e^-$

Cathode: $1/2\ O_2 + 2\ H_3O + 2e^- \Leftrightarrow 3\ H_2O$

Overall reaction: $H_2 + 1/2\ O_2 \Leftrightarrow H_2O$

The low temperature PEMFC achieves the highest power density of 0.3 to over 1 W/cm^2 compared to other fuel cell types. It is also characterized by a low operating temperature and fast start-up and shut-off capability, as well as a high degree of efficiency in the partition portion, which makes it suitable for both stationary and portable or automotive systems. Disadvantages are the cost of the precious metals of the catalyst (platinum, ruthenium) and its sensitivity to carbon monoxide and sulfur compounds, with a high purity of the gases used being required. Further, when using NT-PEMFC, it is necessary

to moisten the reactants, especially at higher operating temperatures, in order to prevent the membrane from drying out. The PEMFC single cell consists of two half cells (anode/cathode) with the half cells being separated by a polymer electrolyte membrane. This membrane is gas-tight and electrically insulating. On the anode side, the oxonium, hereinafter simply referred to as proton, is generated, wherein the protons are passed over the membrane to the cathode. To ensure the best possible proton transport across the membrane, the membrane must be moistened. The better the membrane is moistened, the lower the membrane resistance. Adjacent to the membrane, the cathode electrode and anode electrode are arranged in the form of the catalyst layer, for which mostly platinum or platinum alloys are used. The membrane and the electrode are usually manufactured industrially as a component unit and stabilized by a gas diffusion layer. The task of the gas diffusion layer (GDL) essentially consists of the homogeneous distribution of the gaseous reactants to the catalyst layer and the removal of the product water generated on the cathode side. Adjacent to the GDL, a flow distribution plate with flow channels which is also referred to as flow field, is arranged on both the anode and cathode sides. The flow field is to achieve as homogeneous a distribution of the reactants over the entire active area of the PEMFEC as possible. In a single cell adjacent to the flow distribution plate, the current collector plate is arranged to transport the electrodes generated on the anode side via the generated circuit and the electrical load to the cathode. However, in order to achieve the highest possible overall performance with higher total voltages, the respective single cells are formed into a fuel stack (fuel cell stack) and connected in series. Since, in the case of a stack, the flow distribution plates of the anode and the cathode of adjacent single cells are in direct contact with one another, the two plates are combined to form so-called bipolar plates, in which the anode-side flow field is located on one side and the cathode-side flow field is located on the other side. The bipolar plate is also made of an electrically conductive material in order to transport the electrodes from the anode to the cathode of the next cell.

The mode of operation of a PEMFEC is shown in Fig. 1. The fuel cell according to Fig. 1 is composed of a cathode and an anode with a membrane being arranged in between. The purpose of the polymer electrolyte membrane is to transport the protons produced on the anode side to the cathode. Thus, the membrane must have very high proton conductivity. The membrane between the anode and the cathode serves to separate the two half-cells

firstly by having very low electron conductivity and secondly by being virtually impermeable to hydrogen and oxygen. The membrane is able to store liquid water, which causes the membrane to swell, the membrane being able to increase its volume by up to 22%. Due to the swelling of the membrane, water-filled clusters are formed which are connected to each other via channels of about 3 nm. Ultimately, the swelling of the membrane lowers the energy barrier for proton migration and thus membrane resistance. The diameter of the water-filled clusters strongly depends on the water content of the membrane, and as the water content decreases, the permeability of the cluster also decreases, thereby exposing the protons to greater electrostatic interaction and increasing the membrane resistance so that the power of the fuel cell is reduced. Therefore, the membrane must always be moistened and the temperature must be monitored. To ensure sufficient membrane moistening, the reaction gases must be externally moistened at operating temperatures above approximately 50 °C.

The complex structure of the fuel cell according to Fig. 1 results in many possibilities for degradation which have a considerable influence on the performance of the fuel cell as well as on the service life of the fuel cell.

In order to detect such changes or deteriorations of individual components/modules of the fuel cell, the invention provides a method and a device for diagnosing and forecasting the service life of the subassemblies of the fuel cell.

Figs. 2a and 2b show two different exemplary excitation frequencies. In Fig. 2a, the excitation frequency f_n applied to the fuel cell is composed of a sinusoidal frequency f_S and a square wave signal f_R which are in phase with each other, respectively. From the composite single-phase signal results a stronger absolute excitation of the fuel cell, so that the fuel cell is loaded with a large amplitude swing. This normally undesirable load on the fuel cell having a larger alternating signal amplitude, as described in more detail below, results in an increased generation of even harmonics if one or more cells, e. g. by occurring mass transport inhibitions, are in a non-linear region of the characteristic curve. By a simple phase (time) shift of the sine signal f_S, an opposite-phase superposition of the signal fs with the rectangular signal f_R may be generated. Fig. 2b shows such a superposition of a sine signal f_S and a rectangular signal f_R, which are opposite in phase

to one another. That is, for the individual frequencies of the sine signal f_S or the rectangular signal f_R, with which the fuel cell is excited, the same absolute excitation is caused or the same amplitude is used for excitation, as in Fig. 2a. However, in Fig. 2b, when a fuel cell is excited, the absolute excitation with the resulting excitation frequency f_n is lower due to the individual signals being opposite in phase, so that the fuel cell experiences less load, since the total amplitude of the excitation frequencies is lower. That is, in an excitation according to Fig. 2b, the fuel cell is disturbed less and therefore stressed less. Furthermore, the occurrence of even harmonics with increased sensitivity and accuracy may be determined by successively switching the supply of the signal F_S between equal and opposite phase, thus improving the detection of cells with non-linear characteristic curve corresponding to reduced cell voltage.

Fig. 3a shows an exemplary equivalent circuit diagram with four different functional components, Y_1, Y_2, Y_3 and Y_4. In the illustrated equivalent circuit diagram, the parallel circuit of R1 and C1 forms the functional component Y_1, which represents, in particular, the cathode-side mass transport. The ohmic resistance R_2 represents the cell resistance, inter alia the membrane resistance, and forms the functional component Y_2. The functional component Y_3 represents the behavior of the fuels at the cathode with the resistance R3 and the capacitor C3. Here, the capacitances C3 and C4 represent the double layer capacitance establishing between the fuel cell cathode and the electrolyte membrane or between the fuel cell anode and the electrolyte membrane, respectively. The remaining functional component Y_4 from the parallel circuit of R4 and C4 represents, as described above, the anode side. The function Y(f) given by the ideal equivalent circuit diagram may be parameterized with the equivalent circuit diagram components contained in the individual functional components.

$$Y(\mathrm{f}) = \frac{1}{\frac{1}{R1} + \frac{1}{Zc1}} + R2 + \frac{1}{\frac{1}{R3} + \frac{1}{Zc3}} + \frac{1}{\frac{1}{R4} + \frac{1}{Zc4}}$$

That is, by changing the parameters for the equivalent circuit diagram components R1, R2, R3, R4, C1, C3 and C4, the profile of the function Y(f) may be changed. By changing the parameters, i. e., by changing the values, it is thus possible to find a curve, respectively, which optimally fits the set of points of the measured impedances for the impedances measured at different times t1, t2, etc. in each case.

Fig. 3b schematically illustrates the classification or grouping of the measured impedances. In this case, a plurality of measured impedances is, respectively, assigned to a functional component. In the high frequency range, i. e., if the capacitances are short-circuited, only the membrane resistance is in effect. Therefore, the measured impedances at high frequencies are located at the start of the semicircle near the origin. The measured impedances, however, increase in their real part at lower frequencies, i. e., starting from 0.001 Ohm up to about 0.005 Ohm and are characteristic for the additional contributions from anode and cathode kinetics as well as for the mass transfer at their low-frequency end.

Figs. 4a to 4c show corresponding Nyquist plots which represents the measured responses to excitation frequencies at different current densities i_1, i_2 and i_3.

Figs. 4a-4c show the negative imaginary part of the measured impedance in Ohm on the Y-axis and the real part of the measured impedance in Ohm on the X-axis, respectively. The Nyquist plot according to Fig. 4a shows different measured impedances at four different times and the function fitted to the measured impedances, respectively.

The inner, almost semicircular, function curve represents the fitted function $Y(t_1)$ for the impedances Zn (t_1) at time t_1. In order to better illustrate the method according to the invention, it should be imagined that the almost semicircular function curve $Y(t_1)$ is not there. Then, only the measured impedances $Z_n(t)$ would be plotted in the Nyquist plots according to Figs. 4a-4c. They each form a set of points. The measured impedances Z_n at time t_1 are indicated by small dark squares, the measured impedances Z_n at time t_2 are indicated by small stars, measured impedances Z_n at time t_3 are indicated by small dashes (-) and the measured impedances Z_n at time t_4 are indicated by small light squares.

By means of the proposed data regression, for example based on the method of least squares, a function curve $Y(t_1)$ for the function of the equivalent circuit diagram shown in Fig. 3a is now generated for the measured impedances Z_n at time t_1 by changing the parameters, i. e., the equivalent circuit diagram components R and C in their values such that they result in a function $Y(t_1)$ which is as optimally as possible fitted to the set of

points of the measured impedances $Z_n(t_1)$. That is, based on the data regression, specific values for the individual equivalent circuit diagram components can be determined.

For example, in the measurement of the impedances $Z_n(t_1)$, an almost semi-circular curve of the function Y_n (t_1) is apparent. In the front region of the X-axis, the measured impedances at high frequencies are plotted, with the low frequencies being plotted in the rear region of the X-axis, which is the real part of the impedances.

The distance from the zero point to the imaginary intersection of the almost semicircular function curve with the X-axis shows the cell resistance at high frequencies, whereas the cell resistance at low frequencies is shown on the right side of the almost semicircular function curve. According to the equivalent circuit diagram shown in Fig. 3a, for example, the resistances R1, R3 and R4 provided with a capacitor connected in parallel are short-circuited at high frequencies such that only the resistance R2 takes effect. This resistance represents the total ohmic cell resistance, which however consists predominantly of the membrane resistance. Typical values for the ohmic resistance R2 for a cell having an active area of 100 cm^2 are between 0.0004 and 0.002 Ohm. This corresponds to a sheet resistance of 0.04 to 0.2 Ohm cm^2.

In Fig. 4a, a plurality of function curves is shown, which function curves have been determined at four different times t_1 to t_4, respectively, based on measurements of impedances at a current density i_1 = 10A, wherein, by means of the Nyquist plot, it is possible to recognize that the fuel cell is subject to a change that results from aging processes.

For example, when comparing the curve $Y_n(t_1)$ with $Y_n(t_4)$ in Fig. 4a it can be seen that, on the one hand, the cell resistance R2 increases at high frequencies in the left-hand region of the semicircles. However, the increase in cell resistance R2 becomes even clearer when comparing the two measurements t_1 and t_4 at low frequencies (i. e., on the right side of the semicircle) at which the value of the cell resistance R2 increases from 0.0045 to 0.0062 Ohm. This is a clear sign that the cell resistance R2 increases with increasing operating time. This is mainly due to an increase in membrane resistance, which in turn increases, e. g. by the inclusion of metal ions instead of H^+ ions. Another

reason (further explained here only for the sake of completeness) may be that certain areas of the cell are deactivated by aging, that therefore only a part of the active area is available, and that therefore the ohmic resistance is increasing taking into account the entire area of the cell. The increase in the membrane resistance causes the voltage drop across the membrane to increase, as a result of which the output voltage or operating voltage of the fuel cell decreases. When the operating voltage of the fuel cell falls below a predetermined value, e. g. 0.6 V, the fuel cell has reached the end of its service life, because it cannot reach the specified voltage value (and thus the required power and/or the required efficiency). The measurements of the impedances and also the fitted function curves from the times t2 and t3 are almost identical, which is due to the operating conditions which hardly stress the fuel cell in this operating period. In the legend of Fig. 4a, the time intervals between the measurements of $Z(t_1)$, $Z(t_2)$, $Z(t_3)$ and $Z(t_4)$ can be seen. The first measurement was performed on March 17, the second measurement on May 12, the third measurement on June 2, and the fourth measurement on June 9. Between May 12 and June 2, there is no big change, but from June 2 until June 9, i. e., in just seven days, a much larger change, i. e., aging, of the fuel cell can be recognized.

Fig. 4b shows response impedances or measured impedances of the fuel cell, to each of which a function Y(t) has been fitted. In Fig. 4B, a current density i_2 of 27 A was measured.

Fig. 4c shows the measured impedances at four different times with curves Y (t) fitted thereto at a current density of i_3 = 35A.

Here, in comparison with the current density of i_1 = 10 A, it can be seen that, as the current density increases, especially at low frequencies, at the time t_4 the mass transfer is intensified e. g. at the gas diffusion layer and consequently results in a reduction in the reactant concentration in the fuel cell electrode, since the pores in the region of the membrane are filled with water, whereby the pore space available for the gas transport decreases and thus the reactant concentration decreases.

In Fig. 4c, a similar effect can be seen as in Fig. 4b.

Figs. 5a to 5d show value plots in which individual parameters R1, R2, R3, R4 and C1, C3, C4 of the equivalent circuit diagram are plotted for different current densities i_1, i_2, i_3 at a particular day, i. e., are shown at the different measuring times t_1-t_4. For example, what can be recognized here is that the membrane resistance, here denoted by R2, decreases at higher current densities. Furthermore, it can be seen, for example, that the cathode-side polarization resistance R3 substantially decreases with the current density (Figs. 5a to 5d), whilst, on the other hand, an increase of the cathode-side polarization resistance R3 over the operating period is observed, which can be interpreted as reduced catalytic activity and thus as occurred aging of the cell. This can be taken directly from Figs. 6a to 6c.

Figs. 5a-5d and 6a to 6c are based on the following real measurements.

Table 1

Current density	EQV_comp.	a1	b1	f(t), t=1	f(t), t=40	f(t), t=80
10	C1	1,46E-03	2,82	2,821460	2,878400	2,936800
27	C1	1,06	-15	-13,940000	27,400000	69,800000
35	C1	1,17	-17,4	-16,230000	29,400000	76,200000
10	R1	2,95E-06	0,0033	0,003303	0,003418	0,003536
27	R1	-9,07E-06	0,00148	0,001471	0,001117	0,000754
35	R1	-6,38E-06	0,00111	0,001104	0,000855	0,000600
10	R2	2,38E-06	0,000584	0,000586	0,000679	0,000774
27	R2	3,23E-06	0,000531	0,000534	0,000660	0,000789
35	R2	3,32E-06	0,000508	0,000511	0,000641	0,000774
10	C3	-2,25E-02	4,45	4,427500	3,550000	2,650000
27	C3	-1,94E-02	3,77	3,750600	2,994000	2,218000
35	C3	-1,63E-02	3,44	3,423700	2,788000	2,136000
10	R3	1,03E-05	0,000503	0,000513	0,000915	0,001327
27	R3	2,30E-05	0,0000374	0,000060	0,000957	0,001877
35	R3	1,58E-05	0,00016	0,000176	0,000792	0,001424
10	C4	1,52E-02	0,994	1,009200	1,602000	2,210000
27	C4	2,33E-02	0,445	0,468300	1,377000	2,309000
35	C4	2,24E-02	0,42	0,442400	1,316000	2,212000
10	R4	-4,06E-07	0,000168	0,000168	0,000152	0,000136
27	R4	1,48E-06	0,000131	0,000132	0,000190	0,000249
35	R4	5,31E-07	0,000159	0,000160	0,000180	0,000201

The linear equation elements a and b can be taken from Table 1. In addition, the parameter value f(t) of the individual equivalent circuit diagram components C1-C4 and R1-R4 is given at different times. In column 5, the parameter values for t = 1 (day 1), in column 6 the parameter values for t = 40 (day 40), and in column 7 the parameter values for t = 80 (day 80) are indicated. The first column lists the different current densities.

Table 2

Sorted by current i, then by time t									
	i	Time	R1	C1	R2	R3	C3	R4	C4
17_03_ _10a_2	10	1	0,00330	2,85	0,000602	0,00053	4,39	0,000166	1,02
12_05_ _10a_2	10	57	0,00355	2,83	0,000675	0,00100	3,31	0,000151	1,76
02_06_ _10a_2	10	78	0,00318	2,88	0,000754	0,00139	2,52	0,000130	2,44
09_06_ _10a_2	10	85	0,00381	3,05	0,000829	0,001350	2,59	0,00014	2,10
17_03_ _27a_2	27	1	0,00141	2,44	0,000555	0,00025	3,79	0,000157	0,57
12_05_ _27a_2	27	57	0,00121	4,72	0,000659	0,00078	2,58	0,000144	1,47
02_06_ _27a_2	27	78	0,00053	35,29	0,000767	0,00181	2,14	0,000233	2,27
09_06_ _27a_2	27	85	0,00078	132,70	0,000858	0,00239	2,29	0,000316	2,62
17_03_ _35a_2	35	1	0,00111	2,44	0,000524	0,00023	3,47	0,000173	0,40
12_05_ _35a_2	35	57	0,00071	8,52	0,000668	0,00090	2,39	0,000156	1,84
02_06_ _35a_1	35	78	0,00072	12,67	0,000741	0,00133	2,05	0,000168	2,16
09_06_ _35a_2	35	85	0,00050	165,10	0,000834	0,00167	2,24	0,000255	2,23

In Table 2, the parameter values of the individual equivalent circuit diagram components C1-C4 and R1-R4 are sorted by current density and time. The corresponding graphical representations for the three different current densities i = 10 A, i = 27 A, and i = 35 A can be found in Figs. 6a-6c.

Table 3

Sorted by time, then by current									
	I	Time	R1	C1	R2	R3	C3	R4	C4
17_03_ _10a_2	10	1	0,0033019	2,854	0,00060211	0,0005332	4,388	0,00016616	1,02
17_03_ _27a_2	27	1	0,0014138	2,436	0,00055451	0,0002501	3,793	0,00015737	0,56913
17_03_ _35a_2	35	1	0,001109	2,439	0,00052371	0,00023468	3,473	0,00017283	0,39594
12_05_ _10a_2	10	57	0,003548	2,831	0,00067479	0,0010045	3,314	0,00015092	1,759
12_05_ _27a_2	27	57	0,0012142	4,717	0,00065872	0,00078457	2,582	0,00014429	1,468
12_05_ _35a_2	35	57	0,00070953	8,518	0,00066845	0,00090028	2,387	0,00015562	1,836
02_06_ _10a_2	10	78	0,0031764	2,883	0,00075446	0,0013912	2,516	0,00013017	2,443
02_06_ _27a_2	27	78	0,00053021	35,29	0,00076733	0,0018058	2,139	0,00023326	2,265
02_06_ _35a_1	35	78	0,0007174	12,67	0,0007411	0,0013256	2,045	0,00016828	2,161
09_06_ _10a_2	10	85	0,0038141	3,046	0,000829	0,0013497	2,593	0,00013529	2,103
09_06_ _27a_2	27	85	0,00077583	132,7	0,0008582	0,0023891	2,289	0,00031644	2,619
09_06_ _35a_2	35	85	0,00049949	165,1	0,00083422	0,0016685	2,241	0,00025501	2,234

In Table 3, the parameter values of the individual equivalent circuit diagram components C1-C4 and R1-R4 are sorted by time and then by current density. The corresponding graphical representations for the four different times of day 1, day 57, day 78 and day 85 can be found in Figs. 5a-5d.

Figs. 6a to 6c show the parameters determined from the function determination or data regression in terms of their time dependence at different current densities. Thus, Fig. 6a shows the time profile of the equivalent circuit diagram components at a current density of i_1 = 10A, the parameter values of which are obtained by parameterizing or fitting the curve to the measured impedances. For example, it can be seen here that the mass transfer resistance R1 and the associated capacitance C1 run almost horizontally, without a noticeable slope.

The same applies to the resistance at the anode R4 representing the anode-side polarization resistance.

On the other hand, it can be seen that the capacitance at the cathode C3 drops sharply over the operating time. Thus, by monitoring the slopes of the individual parameters or

the values of the parameters and/or by monitoring maximum values or minimum values, it can be determined whether a fuel cell or its components reach a specific value on a day to be forecast and thus reach or fall below a specific state.

If the measurement is performed at different current densities, as shown in, e. g., Figs. 5a to 5d, regression functions may be provided for each of the equivalent circuit diagram parameters which indicate X (X = R, C, ...) as a function of either current density or both current density and time.

If such a function exists, a value is determined, for example, via the integral equation given above and this value is compared to the currently measured U(i, t). If the deviation exceeds a predefined threshold, this can be interpreted as a change of state of the fuel cell and, for example, an alarm can be triggered and/or a new regression can be started.

For example, the membrane resistance for the operating voltage may be determined by parallel voltage measurements.

In the following, a forecast of the service life based on the method according to the invention is described using the example of cell resistance R2. As a condition for an end of the service life of the fuel cell, for example a maximum ohmic voltage drop of 100 mV at a rated current density of, e. g., 1 A/cm^2 is set. This corresponds to a sheet resistance of 0.1 Ohm cm^2. Assuming a resistance R2 which is constant at higher current densities, according to Fig. 6c with the regression line $R2(t) = 3.32\ 10^{-6}\ t + 5.08\ 10^{-4}$, t = time in days, this results in a service life of 148.2 days, until R2 reaches a value of 0.001 Ohm (0.1 Ohm cm^2 * 100 cm^2 active area) and thus the defined end of service life is reached.

Further embodiments of the invention are conceivable, such as taking the equivalent circuit diagram sum values from R1 to R4 for the corresponding forecast approach. Furthermore, in addition to the continuously performed linear regression of the equivalent circuit diagram parameters, a corridor around this linear regression value may be considered and an alarm signal may be triggered if one of these values breaks out of a

predefined bandwidth ("corridor"), and a new regression with changed forecast values is started and thus the occurrence of event-related aging processes is considered.

The procedure according to the invention has been explained with reference to an equivalent circuit diagram according to Fig. 2. This equivalent circuit diagram is a known simple equivalent circuit diagram according to the prior art. The advantage of the selected equivalent circuit diagram is that it reproduces all the essential components as well as the running processes and that at the same time it keeps the number of variables manageable. According to the procedure described, other equivalent circuit diagrams may also be used and a service life forecast may be performed with analogous methods. These may, e. g., be used for the adjustment at the time t1 and be selected via the accuracy of the fit to the profile in the Nyquist plot.

Furthermore, when fitting Z(i, t), certain values of the parameters may be kept within a reasonable bandwidth in order to increase the accuracy and stability of the fit. Thus, there can be used, e. g., meaningful limit values for the double layer capacitances (C3, C4) in the range of 1 to 10 mF cm^2 and of the resistances R3 and R4 which represent the cathode-side and anode-side resistances of 0.01 to 0.3 Ohm cm^2. Likewise, a narrower limitation of the values is possible in order to obtain a fixed mapping of the equivalent circuit diagram components to the functional components that is stable for every parameter fit.

In Figs. 4a to 4c and also in Figs. 5 and 6, further measurements beyond two measurements in time are shown at further times t3 and t4.

In Fig. 7, the method according to the invention is illustrated by way of example with reference to a flow chart. In step S71, an excitation signal is applied to the fuel cell. Here, the method according to the invention is described only with reference to two measurement times.

The fuel cell excited with an excitation signal outputs a response function in the form of impedances which are measured in step S72. As already described in more detail above,

upon a voltage excitation of the fuel cell the response frequency is measured as a current. Conversely, upon a current excitation, the response in the voltage range is measured.

Here, steps S71 and S72 correspond to the impedance spectroscopy which will not be explained in detail here. That is, after step S72, there is a set of points in a Nyquist plot for time t1.

In a next step S73, there is selected an equivalent circuit diagram representative of the fuel cell which is to be investigated.

Fuel cells basically exhibit a structure as shown in Fig. 1.

With the equivalent circuit diagram shown in Fig. 3a, fuel cells with a required accuracy for a service life forecast may be described very well. However, it is also possible to use other equivalent circuit diagrams in which further functional components of the fuel cell are included and represented by equivalent circuit diagram components.

One possible method of determining a suitable or other equivalent circuit diagram may be that reference function curves are present. With the known reference function curves, it is now attempted to capture the measured set of points of impedances in the Nyquist plot as well as possible without major adjustments to the reference function curve.

With the equivalent circuit diagram matching the reference function curve and the associated function or formula with the functional components of the equivalent circuit diagram of the fuel cell, an adaptation or fitting process to the measured impedances is carried out in step S74 by means of data regression.

Here, the individual parameters from the equivalent circuit diagram are changed in their values such that the function curve fits as optimally as possible to the set of points in the Nyquist plot. As a result, real values or parameters for the equivalent circuit diagram component are obtained, which in turn can be used for the components of the fuel cell represented by the equivalent circuit diagram component.

These parameters are stored in step S75 with time stamp t1. In steps S76 to S79, substantially the steps at time t1 are repeated, with the exception that the selection of an equivalent circuit diagram or a function resulting therefrom is no longer necessary.

Thus, in step S76, the same excitation signal is again applied to the fuel cell. Again, the excitation signal may be composed of different frequency components. In step S77, the response is measured in the form of impedances at the fuel cell and plotted in the Nyquist plot.

Now, by changing the parameters of the equivalent circuit diagram components again, it is attempted to optimally match the function curve to the point set of the impedances at time t2.

This is shown, for example, in Figs. 4a to 4c. The parameters of the equivalent circuit components determined at time t2 are also stored in step S79.

With the various parameters of the equivalent circuit diagram components thus obtained at different times t1, t2, a time dependence of the parameters of the equivalent circuit diagram components may be determined in step S80.

This process is shown in Figs. 6a to 6c.

Referring to Fig. 6a, it is thus possible to determine a regression line for the capacitances or resistances of the equivalent circuit diagram in each case.

In step S81, based on predetermined conditions for the service life forecast such as an operating life, a minimum operating voltage, a limit range of resistance or capacitance values, etc., various forecasts are made with respect to the service life of the fuel cell.

As can easily be recognized in Fig. 6a, by extending the straight line at the desired time it is possible to make statements about the value of the corresponding parameter, which makes it possible to obtain a forecast for the future for individual components of the fuel cell.

Fig. 8 shows a device for forecasting the service life of a fuel cell. Here, the device comprises a fuel cell 800 which is connected, for example, to a load 900. The fuel cell FC provides this load 900 with an operating voltage U_{FC} and supplies a current. The measurement of the impedances is preferably carried out under load, i. e., different load scenarios are defined, whereby the measurements take place at different times under the same load conditions.

The excitation signal f_N is provided by a frequency generator 810 and applied to a fuel cell 800. By means of a measuring unit 820, the impedances at the different times t1, t2 are measured. The measured impedances are then processed in a data regression module 830, so that a function curve Y(f) and corresponding parameters of equivalent circuit diagram components are adjusted to the set of points of the measured impedances Z(f, t) and thus parameter values of the individual equivalent circuit diagram components are determined.

In the evaluation module 830, the parameter values thus obtained for the equivalent circuit diagram components are put into temporal relation to one another and regression functions or regression lines are determined, respectively, with which a service life forecast for the individual components of the fuel cell is possible.

As shown in Fig. 8, modules 810, 820, 830 and 840 may also be present in a measuring and evaluation unit 850.

KRAV

1. Fremgangsmåde til diagnosticering og/eller forudsigelse af levetiden for en brændselscelle, hvor fremgangsmåde omfatter de følgende trin at:

påføre (S71) et exciteringssignal f_n til brændselscellen (800) ved et første tidspunkt t_1,

detektere (S72) impedanser $Z_n(f_n, t_1)$ ved exciteringsfrekvenserne af exciteringssignalet f_n ved det første tidspunkt t_1,

bestemme (S73) en funktion Y(f) for de detekterede impedanser $Z_n(f_n, t_1)$, som indeholder funktionelle komponenter ($Y_1(f)$, $Y_2(f)$, $Y_3(f)$ og $Y_4(f)$) af et forudbestemt ækvivalent kredsløbsdiagram for brændselscellen (800), hvor hver funktionel komponent ($Y_1(f)$, $Y_2(f)$, $Y_3(f)$ og $Y_4(f)$) omfatter mindst én ækvivalent kredsløbsdiagramkomponent (R, C), hvis værdier kan parametreres,

bestemme (S74) mindst én parameter $R(t_1)$, $C(t_1)$ af mindst én ækvivalent kredsløbsdiagramkomponent (R, C) af mindst én funktionel komponent ($Y_1(f)$, $Y_2(f)$, $Y_3(f)$ og $Y_4(f)$) baseret på den bestemte funktion Y(f), der matcher impedanserne $Z_n(f_n, t_1)$, som er detekteret ved det første tidspunkt t_1;

påføre (S76) exciteringssignalet f_n til brændselscellen (800) ved et andet tidspunkt t_2,

detektere (S77) impedanser $Z_n(f_n, t_2)$ ved frekvenserne af exciteringssignalet f_n ved i det mindste ét andet tidspunkt t_2,

bestemme (S78) den mindst ene parameter $R(t_2)$, $C(t_2)$ af den mindst ene ækvivalente kredsløbsdiagramkomponent (R, C) af den mindst ene funktionelle komponent ($Y_1(f)$, $Y_2(f)$, $Y_3(f)$ og $Y_4(f)$) baseret på den bestemte funktion Y(f), der matcher impedanserne $Z_n(f_n, t_2)$, som er detekteret ved det andet tidspunkt t_2;

bestemme (S80) en tidsafhængighed (R(t), C(t)) for den mindst ene parameter $R(t_1, t_2)$, $C(t_1, t_2)$ baseret på parametrene, der er bestemt for det første og det andet tidspunkt t_1, t_2;

detektere (S81) mindst ét tegn på forringelse af en komponent af brændselscellen, der er tildelt den funktionelle komponent i det ækvivalente kredsløbsdiagram, baseret på tidsafhængigheden R(t), C(t) af den mindst ene parameter for mindst én funktionel komponent ($Y_1(f)$, $Y_2(f)$, $Y_3(f)$ og $Y_4(f)$) af det tilsvarende kredsløbsdiagram for brændselscellen,

kendetegnet ved det en hældning af tidsafhængigheden R(t), C(t) af en ækvivalent kredsløbsdiagramkomponent (R, C) bestemmes for at bestemme det mindst ene tegn på forringelse.

2. Fremgangsmåde ifølge krav 1, hvor en funktionel komponent ($Y_1(f)$, $Y_2(f)$, $Y_3(f)$ og $Y_4(f)$) repræsenteres af mindst én ækvivalent kredsløbsdiagramkomponent (R, C) eller en sammenkobling af en flerhed deraf.

3. Fremgangsmåde ifølge et af de foregående krav, hvor bestemmelsen af funktionen Y(f) ud fra de detekterede impedanser $Z_n(f)$ omfatter at gruppere de detekterede impedanser $Z_n(f)$ og at tildele en funktionel komponent ($Y_1(f)$, $Y_2(f)$, $Y_3(f)$ og $Y_4(f)$) med mindst én karakteristisk ækvivalent kredsløbsdiagramkomponent til hver gruppe af impedanser $Z_n(f)$.

4. Fremgangsmåde ifølge et af de foregående krav, hvor en parameteriserbar funktion tildeles til de detekterede impedanser Z_nf) ved hjælp af dataregression for at bestemme en funktion Y(f).

5. Fremgangsmåde ifølge krav 4, hvor de mindste kvadraters metode anvendes som dataregression.

6. Fremgangsmåde ifølge et af de foregående krav, hvor mindst én parameter af funktionen Y(f) er indstillet til en forudbestemt værdi eller et forudbestemt værdiområde med øvre og/eller nedre grænser.

7. Fremgangsmåde ifølge et af de foregående krav, hvorved, et tidspunkt t_x af en overskridelse og/eller en underskridelse af en forudbestemt modstandsværdi eller kapacitansværdi for brændselscellen bestemmes baseret på den bestemte tidsafhængighed (R(t), C(t)) af en ækvivalent kredsløbsdiagramkomponent af det ækvivalente kredsløbsdiagram.

8. Fremgangsmåde ifølge et af de foregående krav, hvor funktionen Y(f) af det ækvivalente kredsløbsdiagram bestemmes for mindst én første strømtæthed (i_1) og en anden strømtæthed (dvs_2).

9. Fremgangsmåde ifølge krav 8, hvorved en funktion $Y_n(f_n, dvs_x)$ af brændselscellen, der er afhængig af strømtætheden (i), bestemmes baseret på funktionerne $Y_n(f_n, dvs_1)$, $Y_n(f_n, dvs_2)$ for den første strømtæthed (dvs_1) og den anden strømtæthed (dvs_2).

10. Fremgangsmåde ifølge et af de foregående krav, hvor målingerne til bestemmelse af impedanserne udføres ved definerede driftspunkter (T, fugtighed, omdannelsesgrad).

11. Fremgangsmåde ifølge et af de foregående krav, hvorved ud over impedanserne $Z_n(f)$ på de forskellige tidspunkter t1, t2 detekteres tilknyttede strøm-/spændingskarakteristika for brændselscellen.

12. Fremgangsmåde ifølge et af de foregående krav, hvor halvbølgeamplituderne af exciteringsfrekvenserne er mindre end 10 mAs/cm^2 med hensyn til det aktive areal af en enkelt celle, og en spændingsamplitude er mindre end 10 mV i forhold til en enkelt celle for ikke at stresse brændselscellen.

13. Indretning til diagnosticering og/eller forudsigelse af levetiden for en brændselscelle, hvor indretningen omfatter:

en frekvensgenerator (810) til at generere og påføre mindst ét exciteringssignal f_n til brændselscellen (800) mindst første og anden tidspunkter t_1, t_2,

en måleenhed (820) til detektering af impedanser $Z_n(f_n, t_1, t_2)$ ved exciteringsfrekvenserne af exciteringssignalet f_n ved i det mindste de første og anden tidspunkter t_1, t_2,

et dataregressionsmodul (830) til at bestemme en funktion Y(f) for impedanserne $Z_n(f_n, t_1)$, der er detekteret ved det første tidspunkt t_1,

hvor funktionen Y(f) indeholder funktionelle komponenter ($Y_1(f)$, $Y_2(f)$, $Y_3(f)$ og $Y_4(f)$) af et tilsvarende kredsløbsdiagram for en brændselscelle (800),

hvor hver funktionel komponent ($Y_1(f)$, $Y_2(f)$, $Y_3(f)$ og $Y_4(f)$) indeholder mindst én ækvivalent kredsløbsdiagramkomponent (R, C), hvis værdier kan parametriseres, og til at bestemme mindst én parameter $R(t)_1$), $C(t_1)$ af den mindst ene ækvivalente kredsløbsdiagramkomponent (R, C) af den mindst ene funktionelle komponent ($Y_1(f)$, $Y_2(f)$, $Y_3(f)$ og $Y_4(f)$) baseret på den bestemte funktion Y(f), der matcher impedanserne $Z_n(f_n, t_1)$ og $Z_n(f_n, t_2)$, der er detekteret ved de første og anden tidspunkter t_1, t_2;

en evalueringsenhed (840) til at bestemme en tidsafhængighed (R(t), C(t)) for den mindst ene parameter (R, C) i det ækvivalente kredsløbsdiagram baseret på parametrene, der er bestemt for de første og anden tidspunkter t1 , t2, og til at detektere mindst ét tegn på forringelse af en komponent i brændselscellen, som er tildelt den funktionelle komponent i det ækvivalente kredsløbsdiagram, baseret på tidsafhængigheden (R(t), C(t)) af mindst én parameter i det ækvivalente kredsløbsdiagram for den mindst ene funktionelle komponent ($Y_1(f)$, $Y_2(f)$, $Y_3(f)$ og $Y_4(f)$),

kendetegnet ved det en hældning af tidsafhængigheden (R(t), C(t)) af en ækvivalent kredsløbsdiagramkomponent (R, C) bestemmes for at bestemme det mindst ene tegn på forringelse.

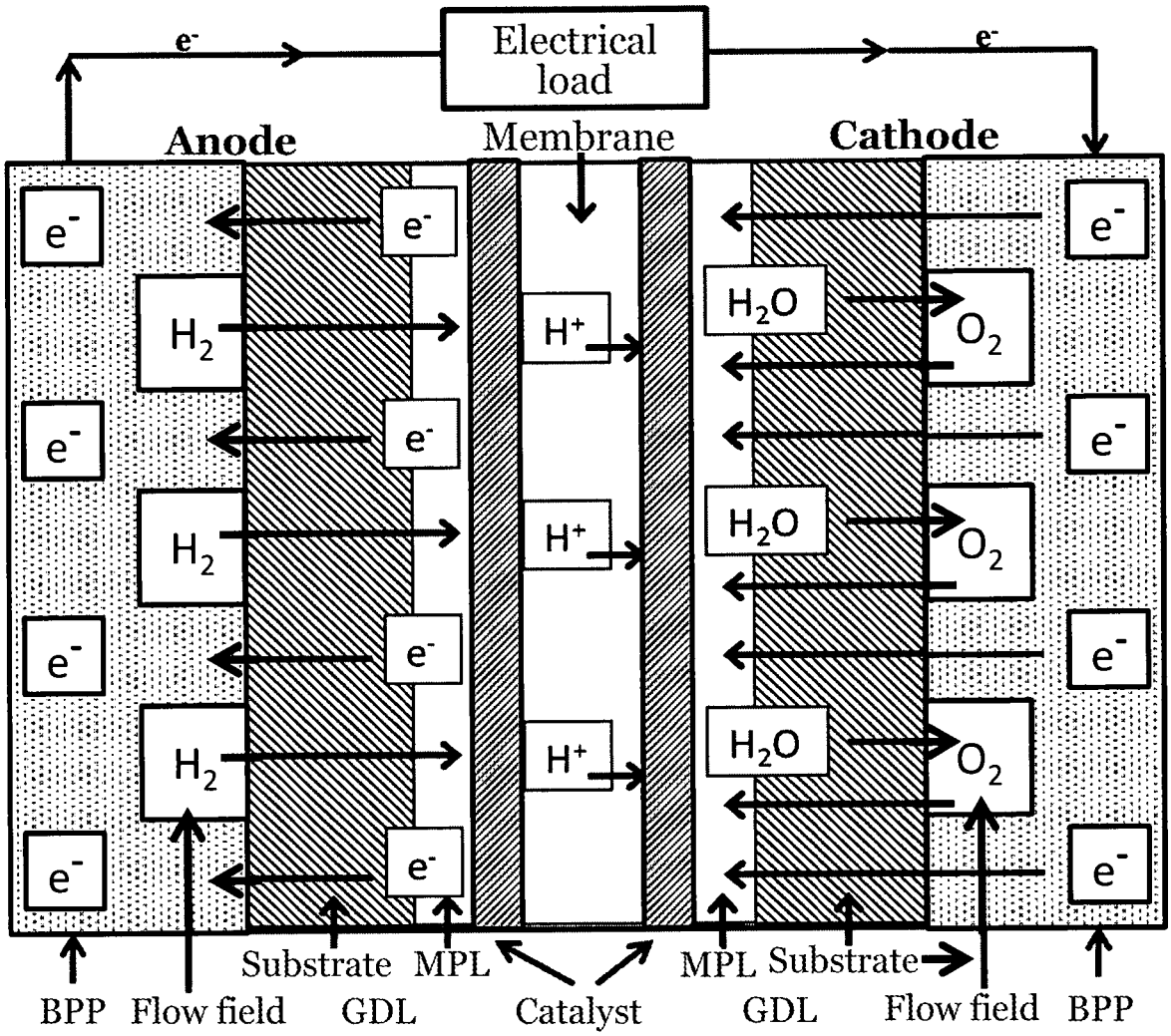
e-
Electrical load
e-
Anode
Membrane
Cathode
e-
H2
e-
H+
H2O
O2
BPP
Flow field
Substrate
GDL
MPL
Catalyst
MPL
Substrate
GDL
Flow field
BPP

Fig. 1

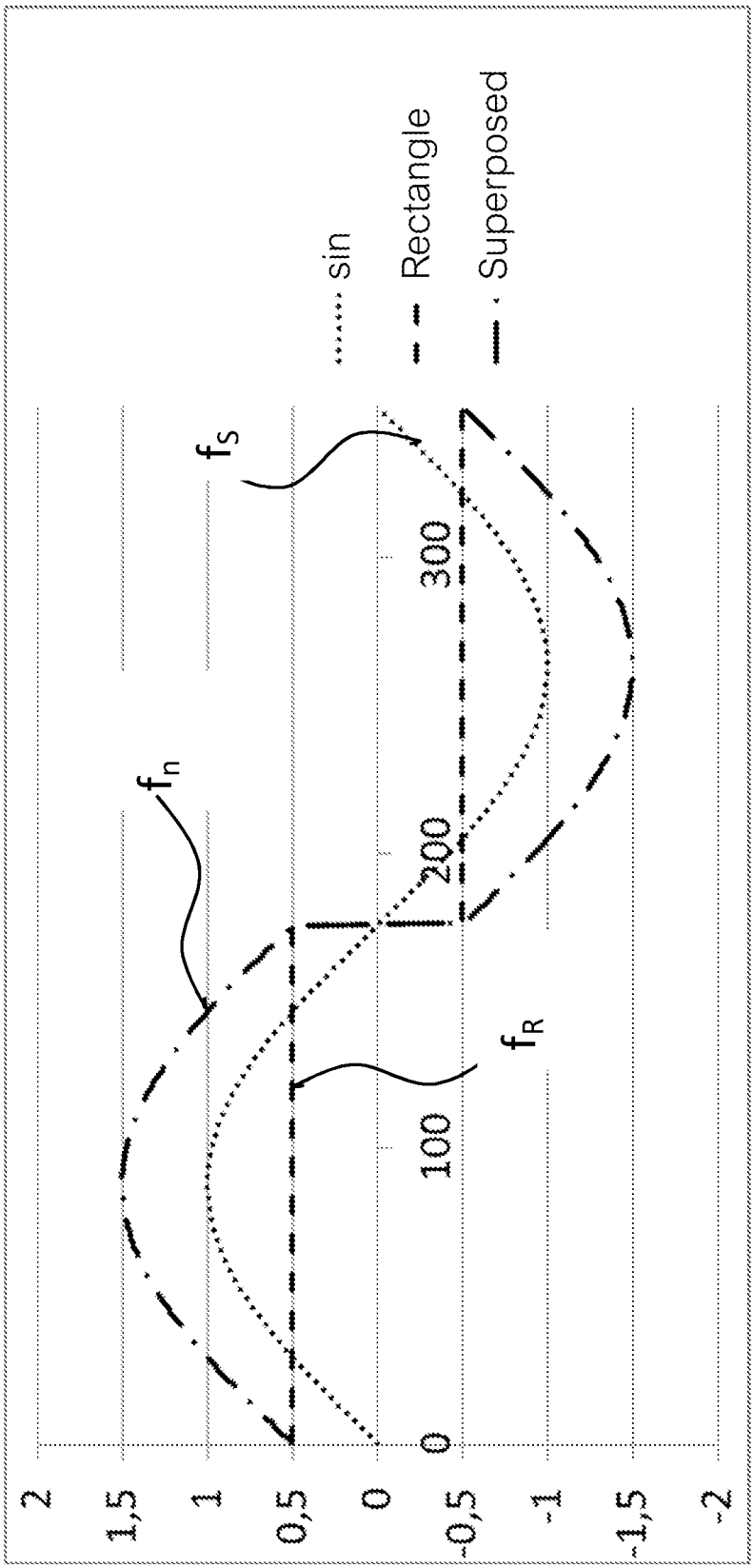
sin
Rectangle
Superposed
f_S
f_n
f_R
300
200
100
0
2
1,5
1
0,5
0
-0,5
-1
-1,5
-2

Fig. 2a

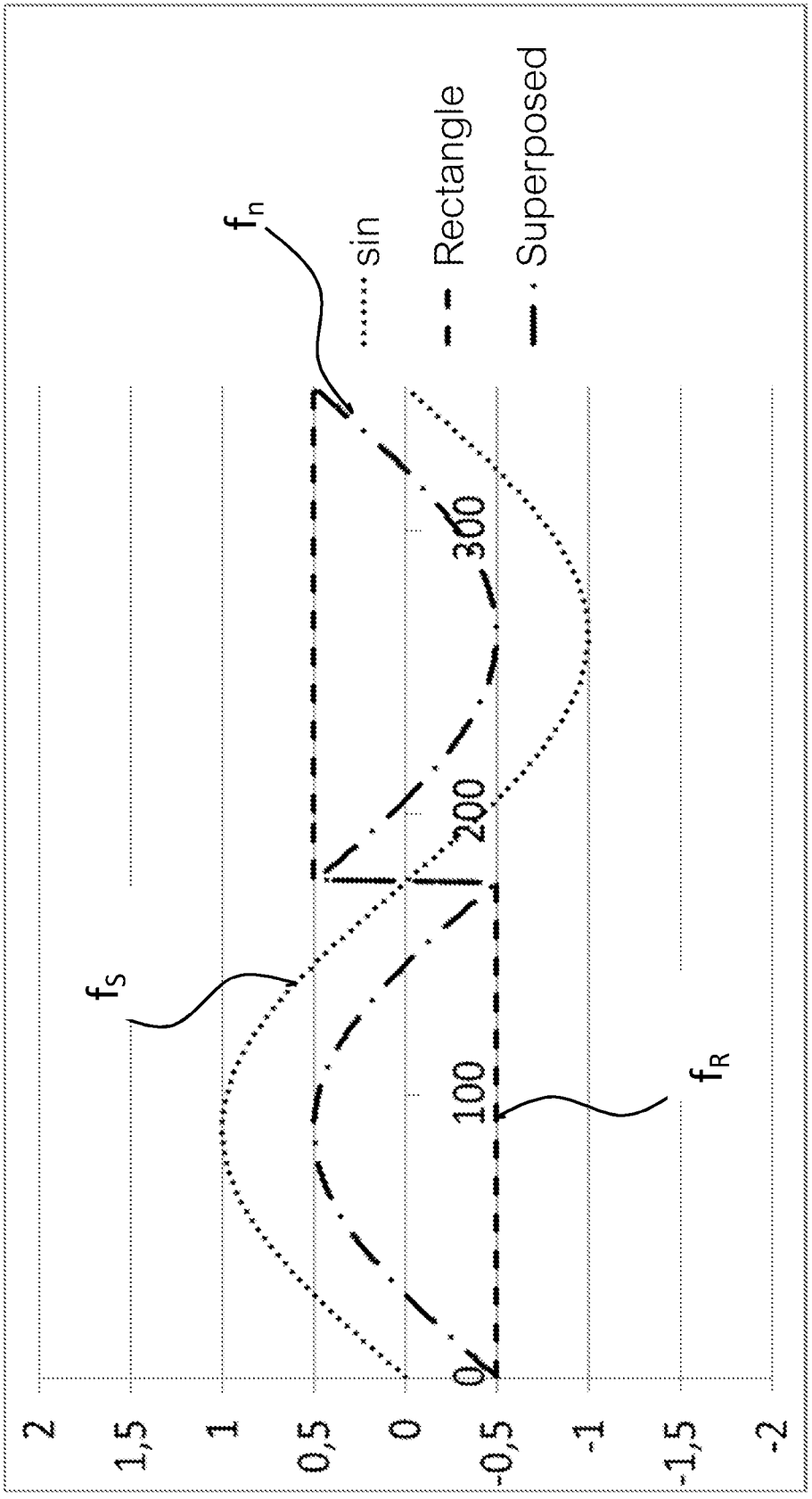
2
1,5
1
0,5
0
-0,5
-1
-1,5
-2
0
100
200
300
f_S
f_n
f_R
sin
Rectangle
Superposed

Fig. 2b

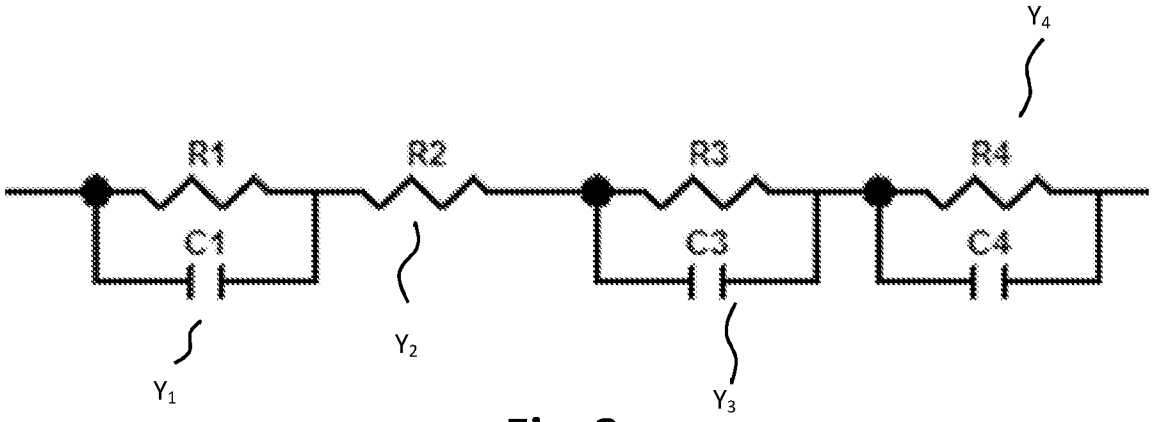
R1
R2
R3
R4
C1
C3
C4
Y1
Y2
Y3
Y4

Fig. 3a

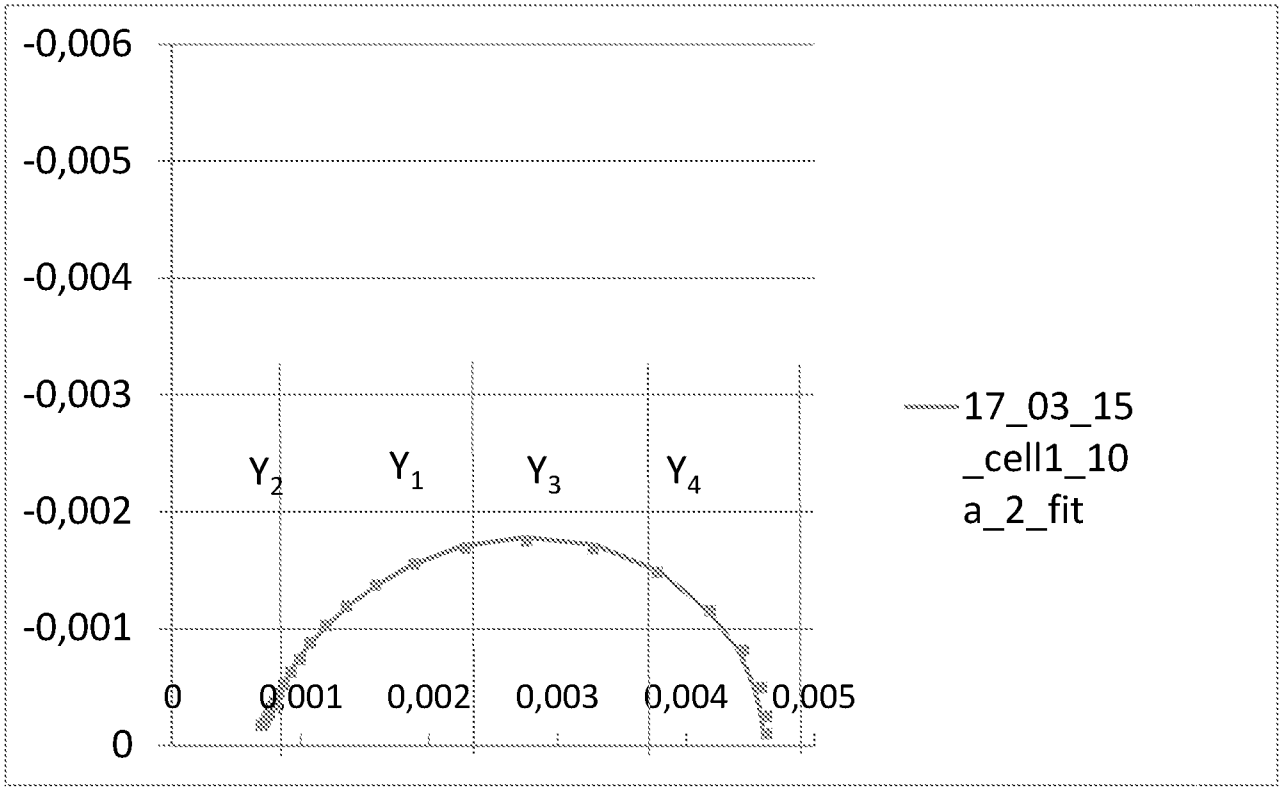
-0,006
-0,005
-0,004
-0,003
-0,002
-0,001
0
0
0,001
0,002
0,003
0,004
0,005
Y2
Y1
Y3
Y4
17_03_15_cell1_10a_2_fit

Fig. 3b

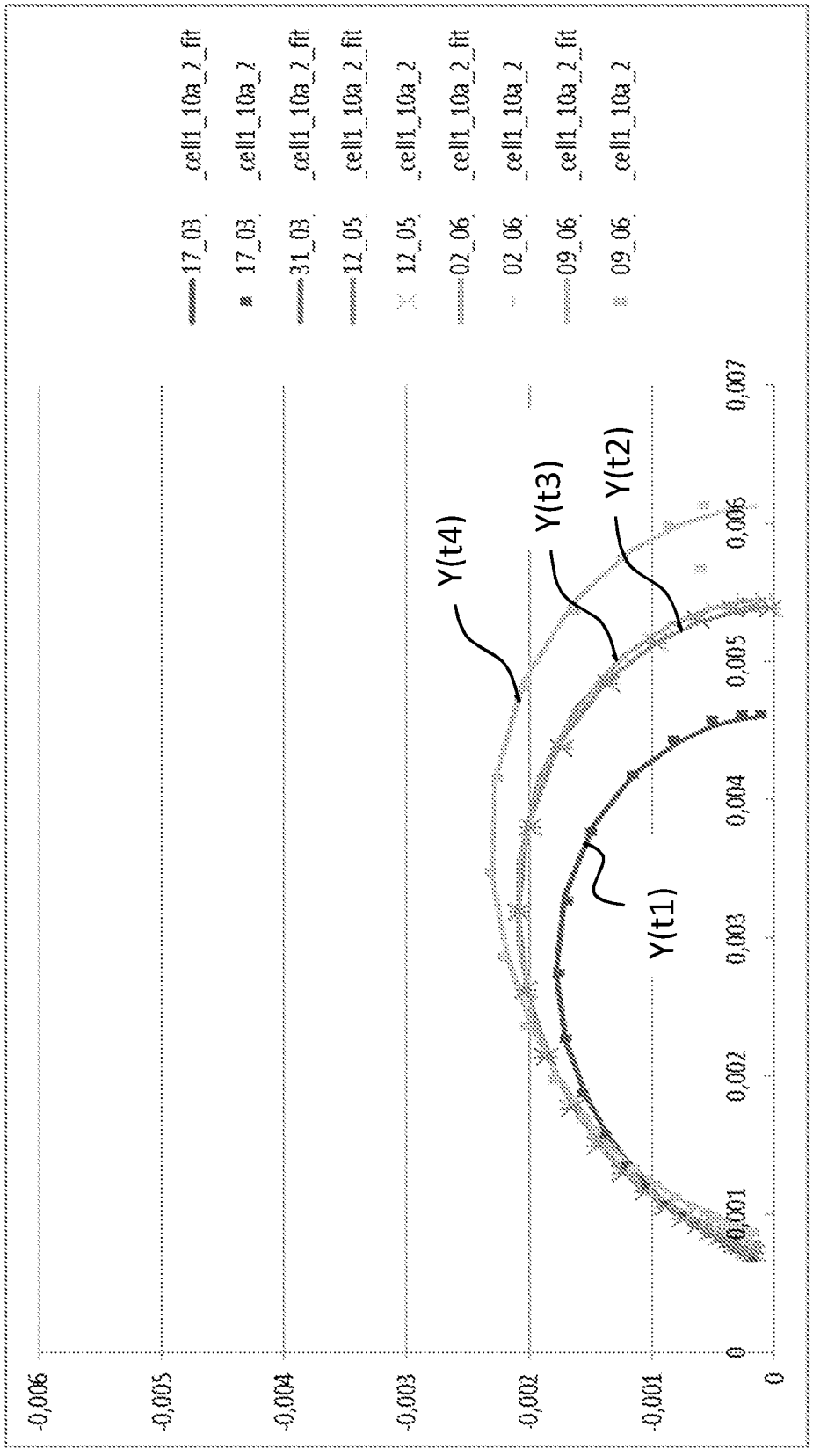
-0,006
-0,005
-0,004
-0,003
-0,002
-0,001
0
0
0,001
0,002
0,003
0,004
0,005
0,006
0,007
17_03 _cell1_10a_2_fit
17_03 _cell1_10a_2
31_03 _cell1_10a_2_fit
12_05 _cell1_10a_2_fit
12_05 _cell1_10a_2
02_06 _cell1_10a_2_fit
02_06 _cell1_10a_2
09_06 _cell1_10a_2_fit
09_06 _cell1_10a_2
Y(t4)
Y(t3)
Y(t2)
Y(t1)

Fig. 4a

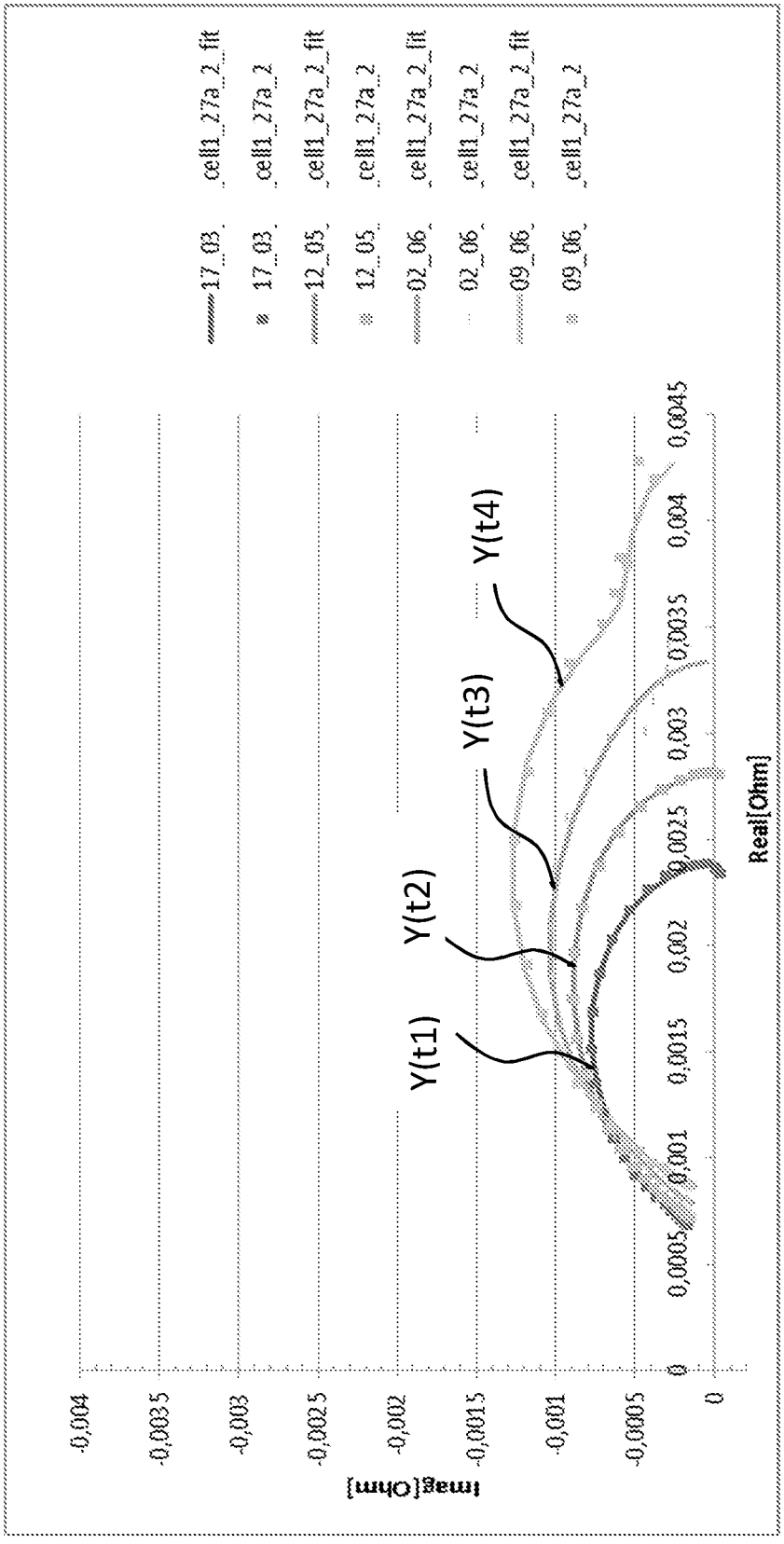
Y(t1)
Y(t2)
Y(t3)
Y(t4)
Real[Ohm]
Imag[Ohm]
17_03_cell1_27a_2_fit
17_03_cell1_27a_2
12_05_cell1_27a_2_fit
12_05_cell1_27a_2
02_06_cell1_27a_2_fit
02_06_cell1_27a_2
09_06_cell1_27a_2_fit
09_06_cell1_27a_2

Fig. 4b

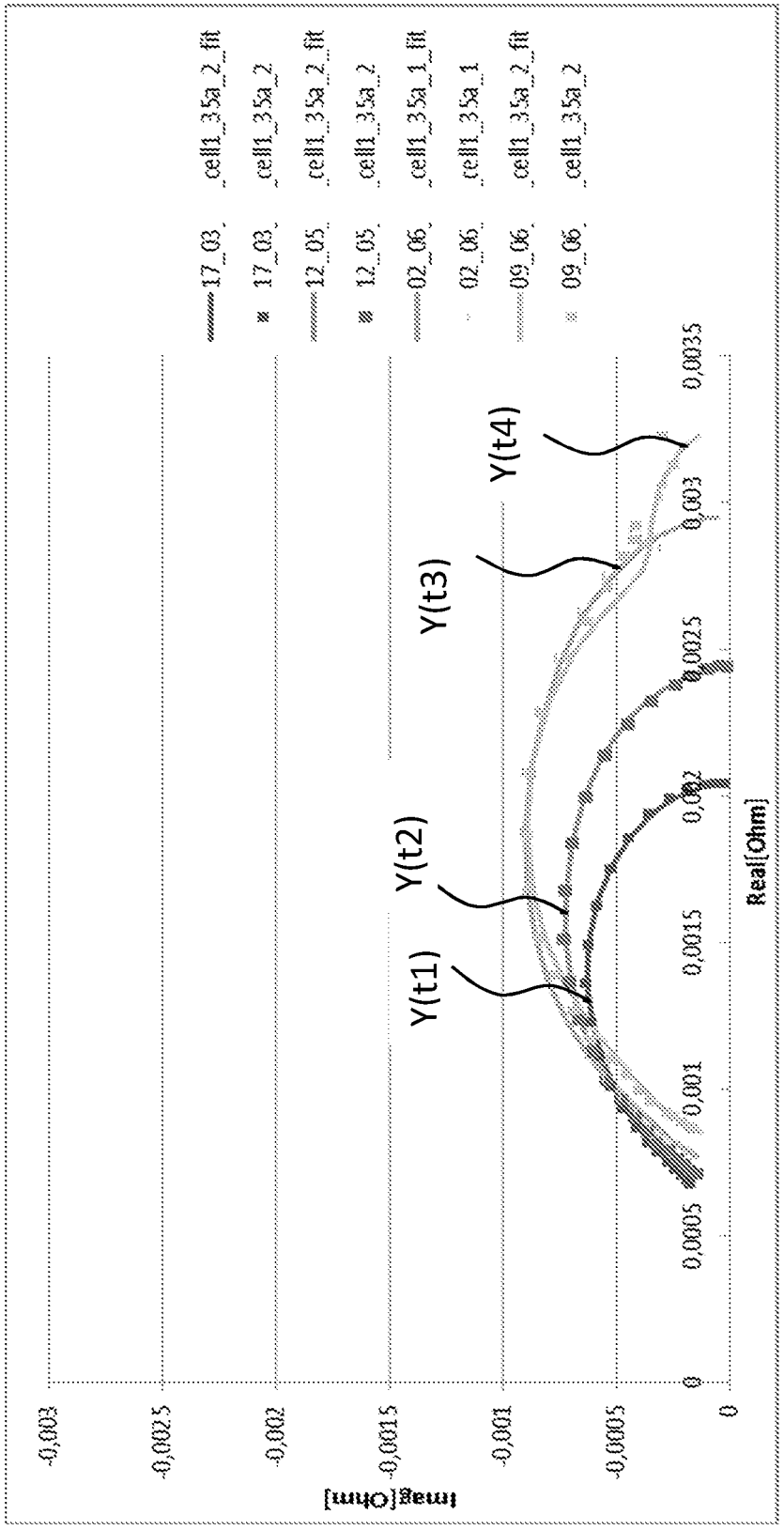
-0,003
-0,0025
-0,002
-0,0015
-0,001
-0,0005
Imag[Ohm]
0
0,0005
0,001
0,0015
0,002
0,0025
0,003
0,0035
Real[Ohm]
Y(t1)
Y(t2)
Y(t3)
Y(t4)
17_03_ _cell1_35a_2_fit
17_03_ _cell1_35a_2
12_05_ _cell1_35a_2_fit
12_05_ _cell1_35a_2
02_06_ _cell1_35a_1_fit
02_06_ _cell1_35a_1
09_06_ _cell1_35a_2_fit
09_06_ _cell1_35a_2

Fig. 4c

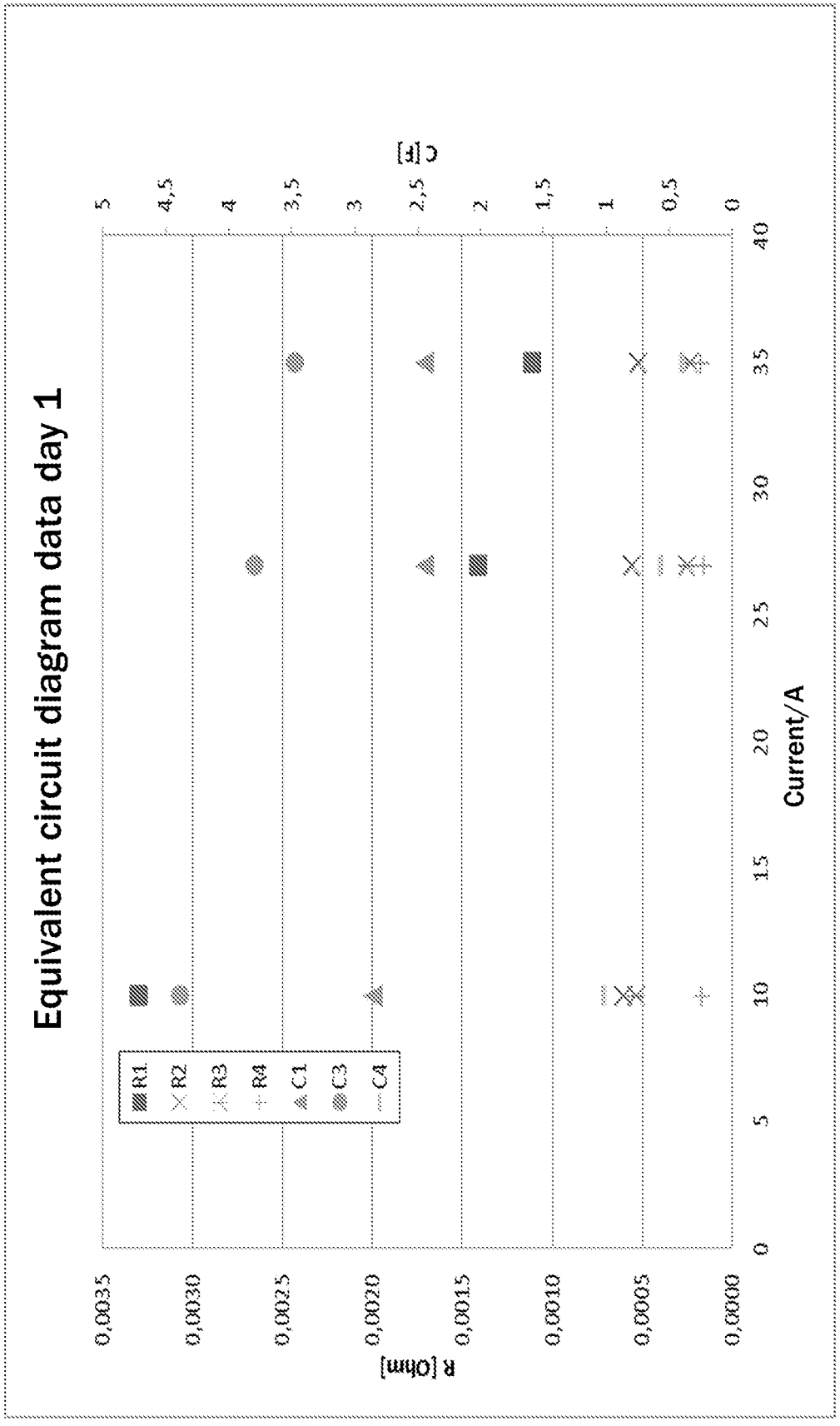
Equivalent circuit diagram data day 1
R [Ohm]
C [F]
Current/A
R1
R2
R3
R4
C1
C3
C4
0,0035
0,0030
0,0025
0,0020
0,0015
0,0010
0,0005
0,0000
5
4,5
4
3,5
3
2,5
2
1,5
1
0,5
0
0
5
10
15
20
25
30
35
40

Fig. 5a

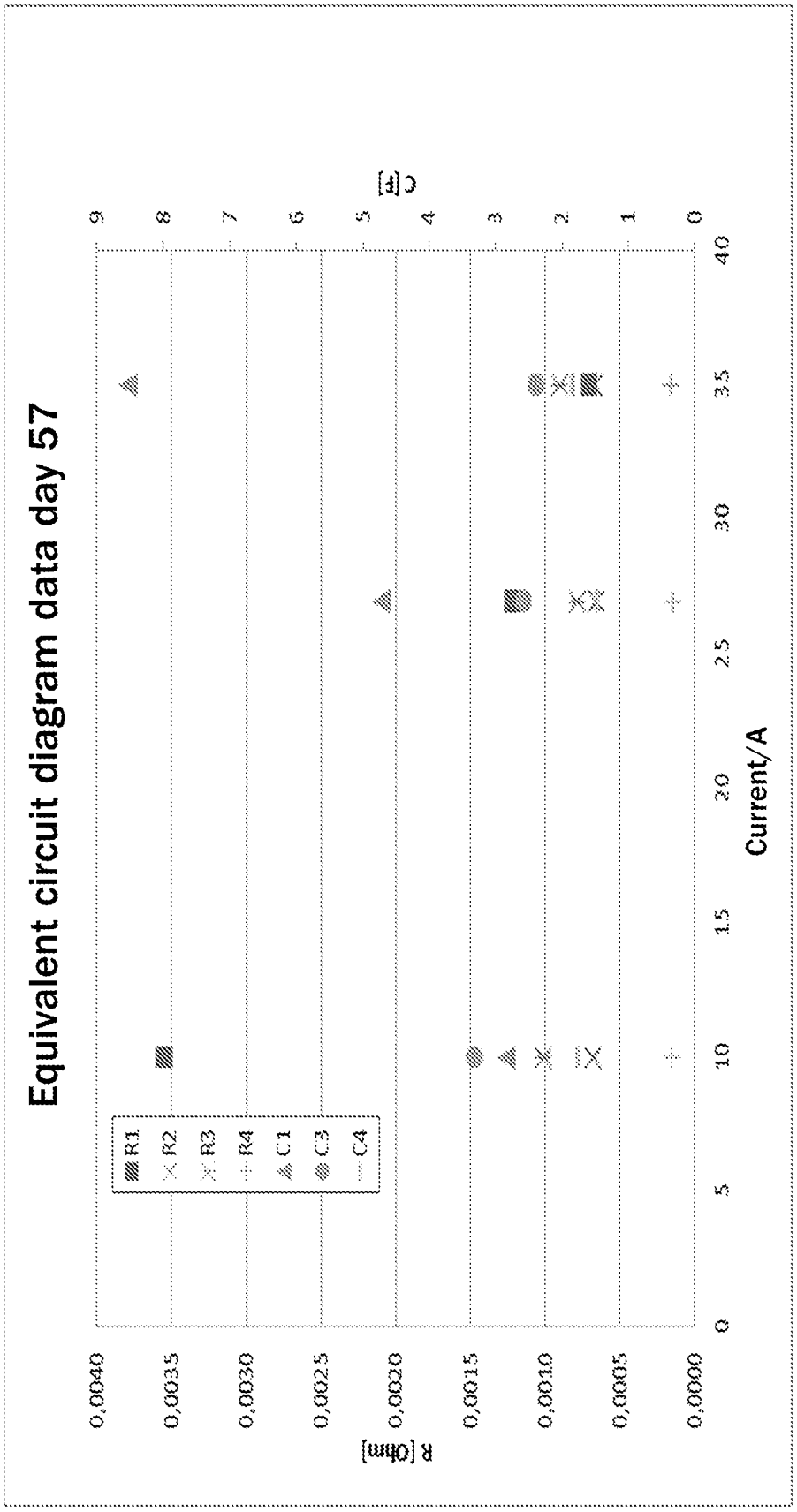
Equivalent circuit diagram data day 57
R [Ohm]
C [F]
Current/A
R1
R2
R3
R4
C1
C3
C4
0,0040
0,0035
0,0030
0,0025
0,0020
0,0015
0,0010
0,0005
0,0000
9
8
7
6
5
4
3
2
1
0
0
5
10
15
20
25
30
35
40

Fig. 5b

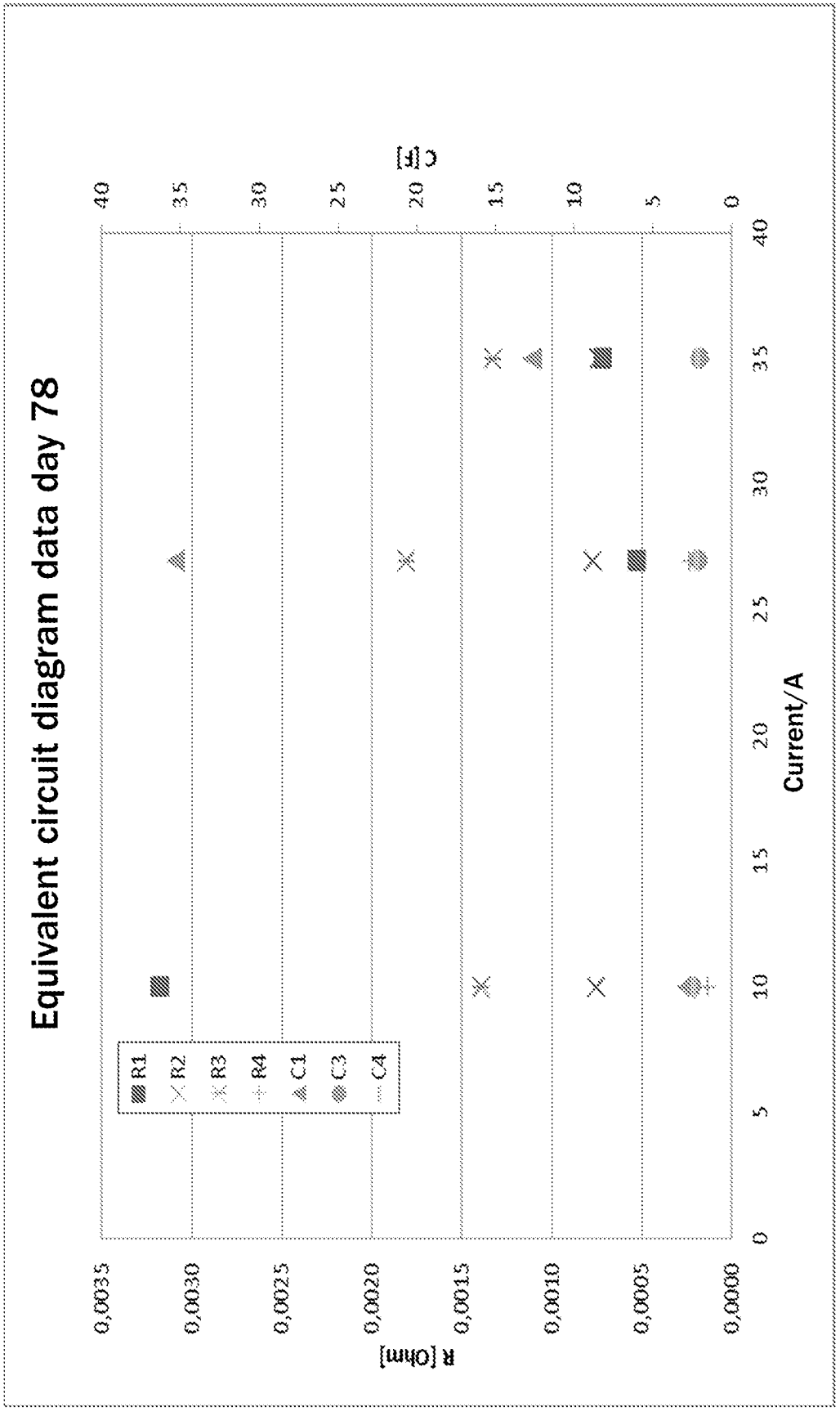
Equivalent circuit diagram data day 78
R [Ohm]
C [F]
Current/A
R1
R2
R3
R4
C1
C3
C4
0,0035
0,0030
0,0025
0,0020
0,0015
0,0010
0,0005
0,0000
40
35
30
25
20
15
10
5
0
0
5
10
15
20
25
30
35
40

Fig. 5c

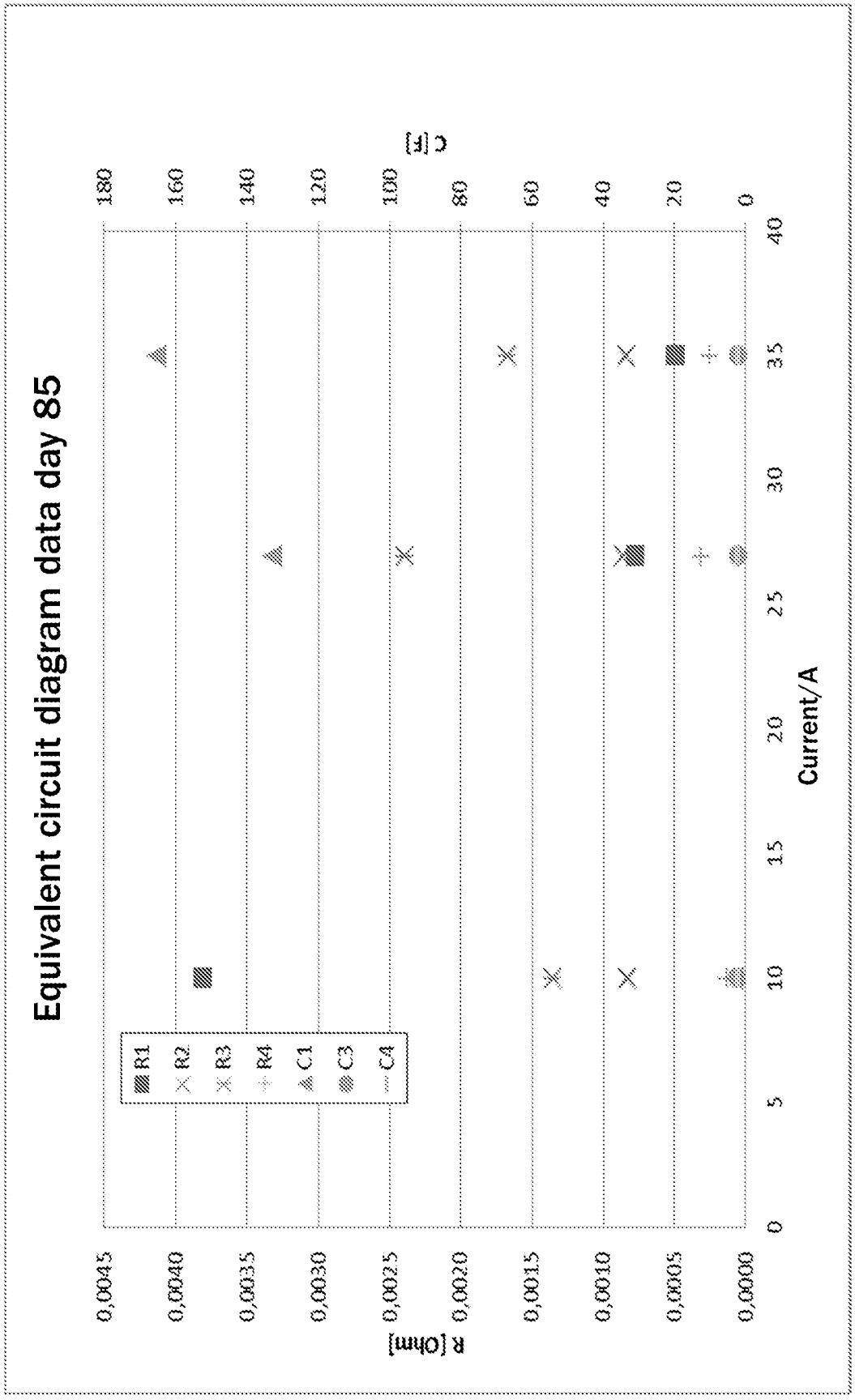
Equivalent circuit diagram data day 85
R [Ohm]
C [F]
Current/A
R1
R2
R3
R4
C1
C3
C4
0,0045
0,0040
0,0035
0,0030
0,0025
0,0020
0,0015
0,0010
0,0005
0,0000
180
160
140
120
100
80
60
40
20
0
0
5
10
15
20
25
30
35
40

Fig. 5d

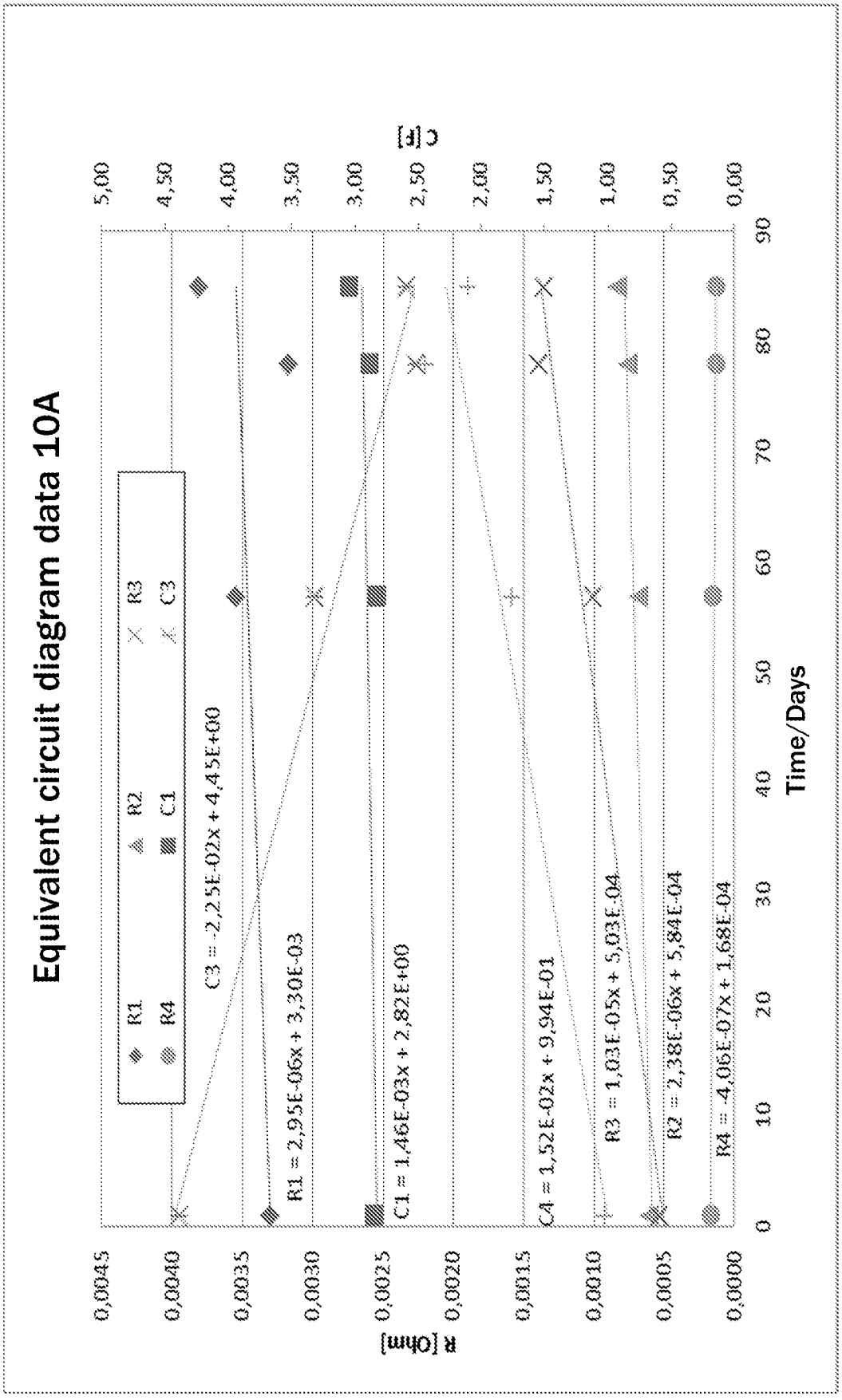
Equivalent circuit diagram data 10A
R1
R2
R3
R4
C1
C3
C3 = -2,25E-02x + 4,45E+00
R1 = 2,95E-06x + 3,30E-03
C1 = 1,46E-03x + 2,82E+00
C4 = 1,52E-02x + 9,94E-01
R3 = 1,03E-05x + 5,03E-04
R2 = 2,38E-06x + 5,84E-04
R4 = -4,06E-07x + 1,68E-04
R [Ohm]
C [F]
Time/Days
0,0045
0,0040
0,0035
0,0030
0,0025
0,0020
0,0015
0,0010
0,0005
0,0000
5,00
4,50
4,00
3,50
3,00
2,50
2,00
1,50
1,00
0,50
0,00
0
10
20
30
40
50
60
70
80
90

Fig. 6a

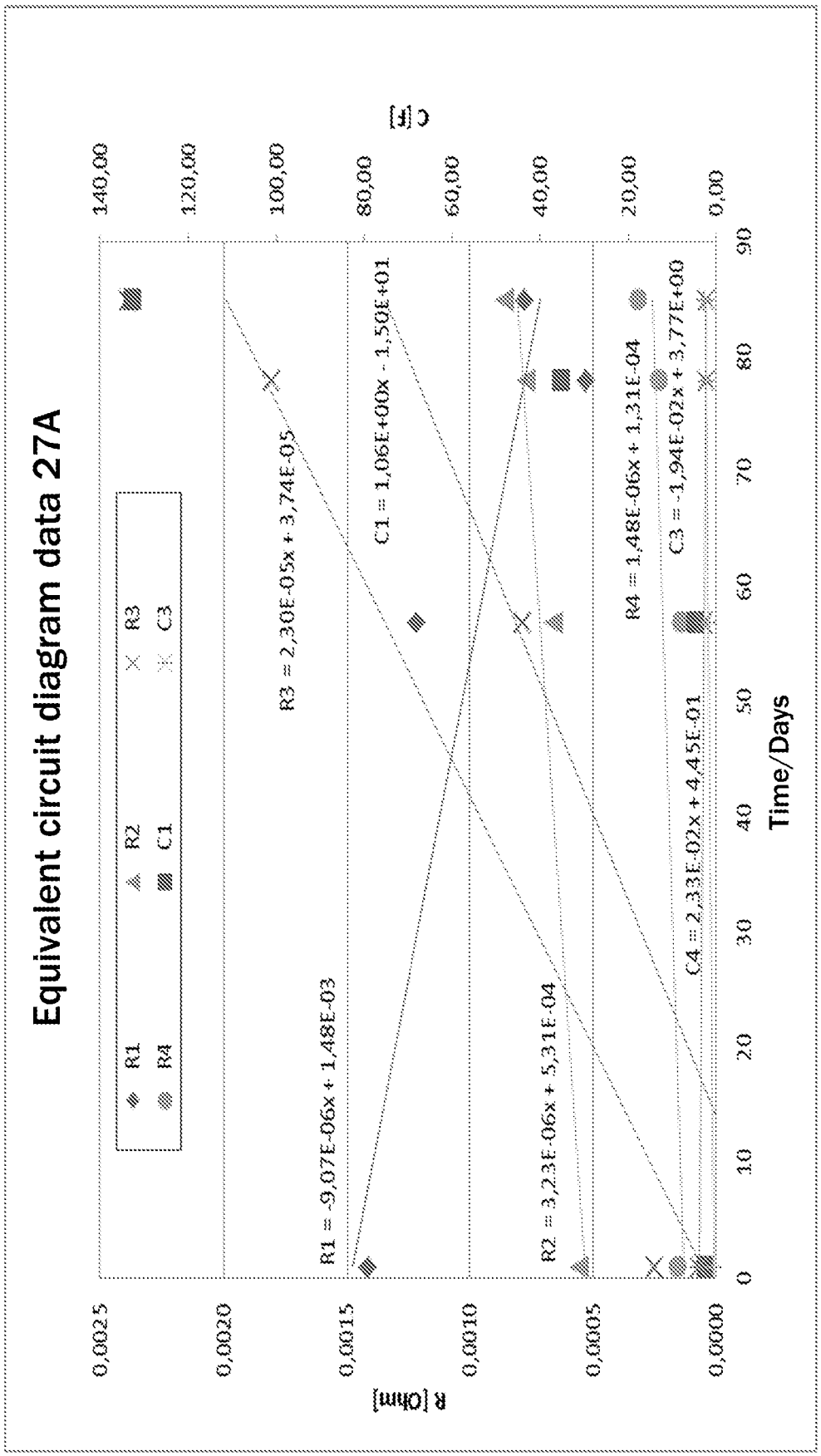
Equivalent circuit diagram data 27A
R1
R2
R3
R4
C1
C3
R1 = -9,07E-06x + 1,48E-03
R2 = 3,23E-06x + 5,31E-04
R3 = 2,30E-05x + 3,74E-05
R4 = 1,48E-06x + 1,31E-04
C1 = 1,06E+00x - 1,50E+01
C3 = -1,94E-02x + 3,77E+00
C4 = 2,33E-02x + 4,45E-01
R [Ohm]
C [F]
Time/Days
0,0025
0,0020
0,0015
0,0010
0,0005
0,0000
140,00
120,00
100,00
80,00
60,00
40,00
20,00
0,00
0
10
20
30
40
50
60
70
80
90

Fig. 6b

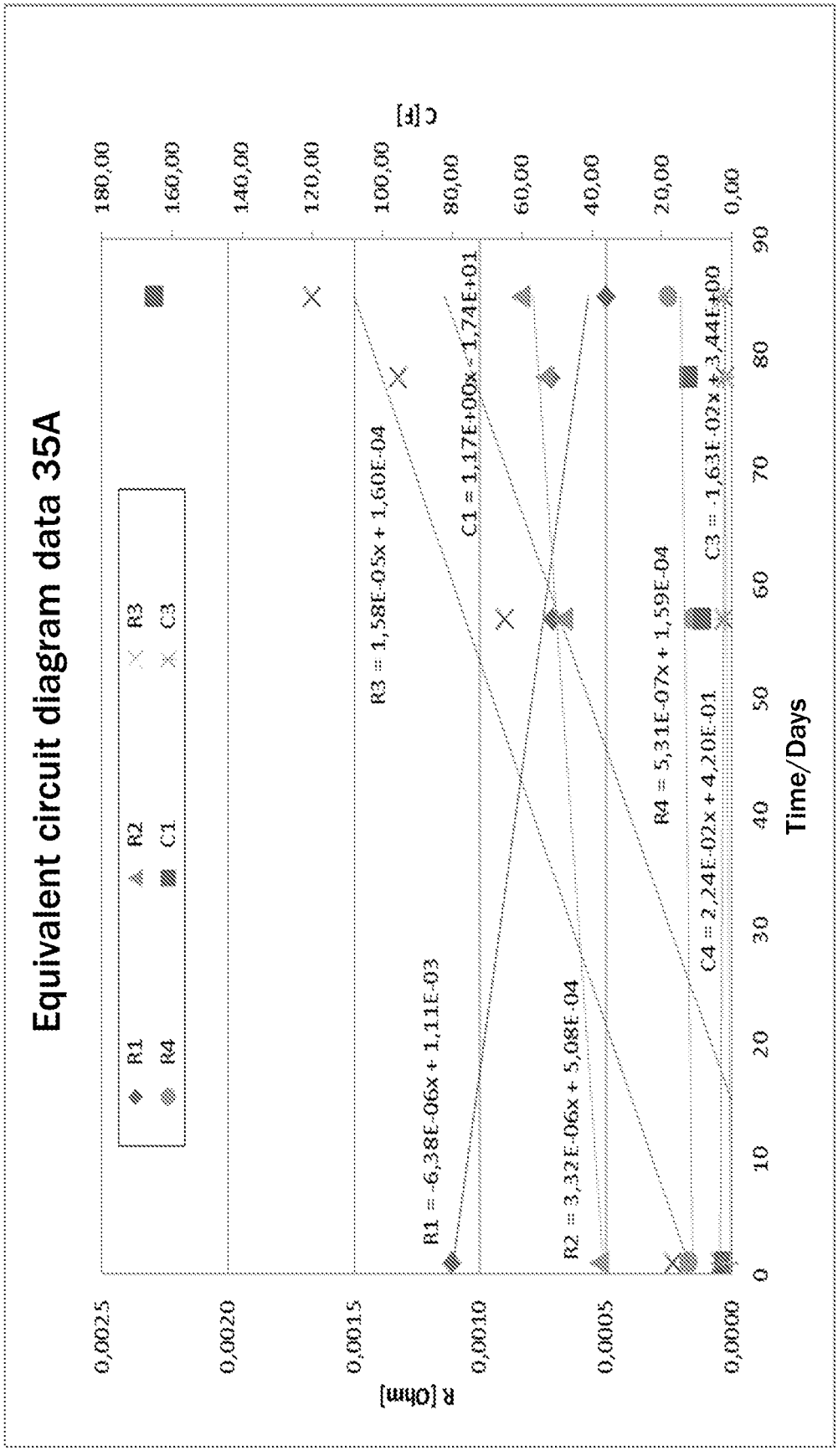
Equivalent circuit diagram data 35A
R1
R2
R3
R4
C1
C3
R1 = -6,38E-06x + 1,11E-03
R2 = 3,32E-06x + 5,08E-04
R3 = 1,58E-05x + 1,60E-04
R4 = 5,31E-07x + 1,59E-04
C1 = 1,17E+00x - 1,74E+01
C3 = 1,63E-02x + 3,44E+00
C4 = 2,24E-02x + 4,20E-01
R [Ohm]
C [F]
Time/Days
0,0025
0,0020
0,0015
0,0010
0,0005
0,0000
180,00
160,00
140,00
120,00
100,00
80,00
60,00
40,00
20,00
0,00
0
10
20
30
40
50
60
70
80
90

Fig. 6c

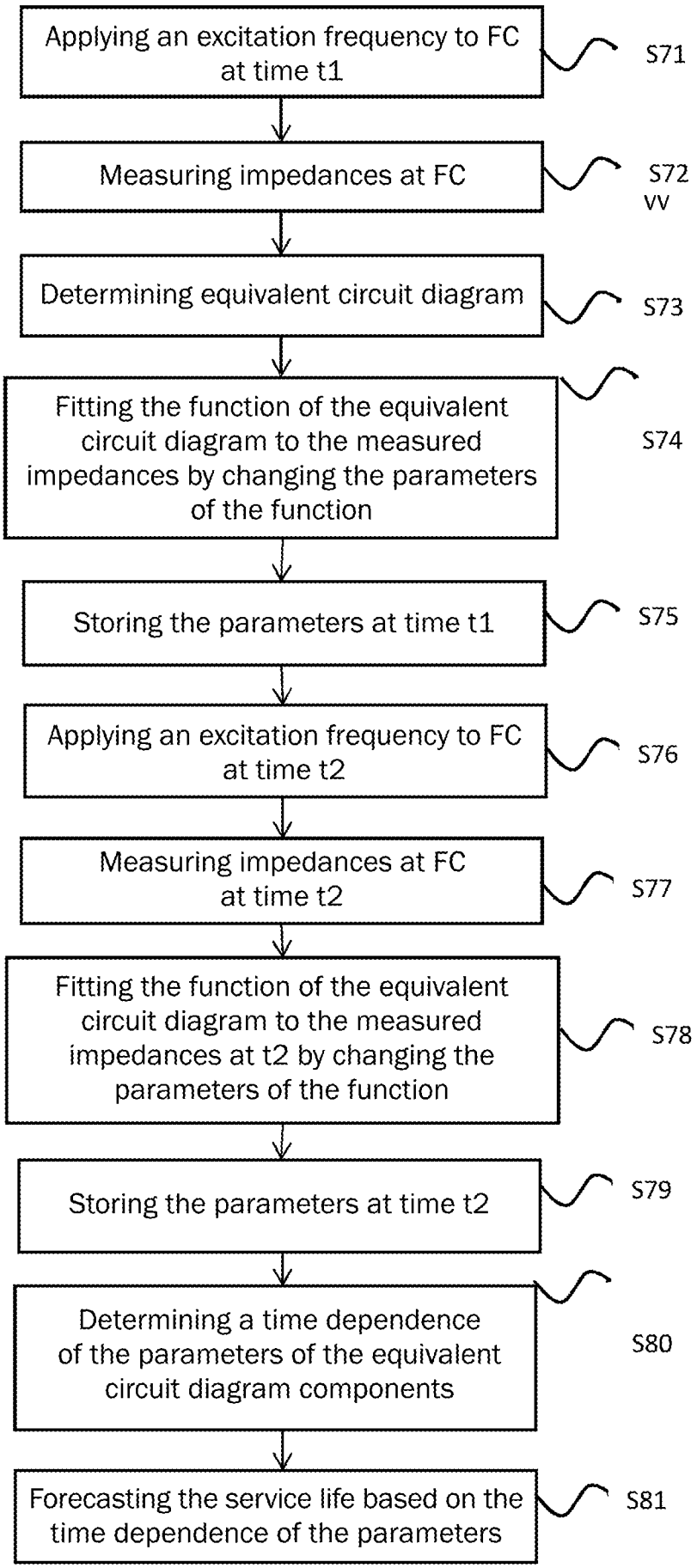
Applying an excitation frequency to FC at time t1
S71
Measuring impedances at FC
S72
Determining equivalent circuit diagram
S73
Fitting the function of the equivalent circuit diagram to the measured impedances by changing the parameters of the function
S74
Storing the parameters at time t1
S75
Applying an excitation frequency to FC at time t2
S76
Measuring impedances at FC at time t2
S77
Fitting the function of the equivalent circuit diagram to the measured impedances at t2 by changing the parameters of the function
S78
Storing the parameters at time t2
S79
Determining a time dependence of the parameters of the equivalent circuit diagram components
S80
Forecasting the service life based on the time dependence of the parameters
S81

Fig. 7

Fig. 8

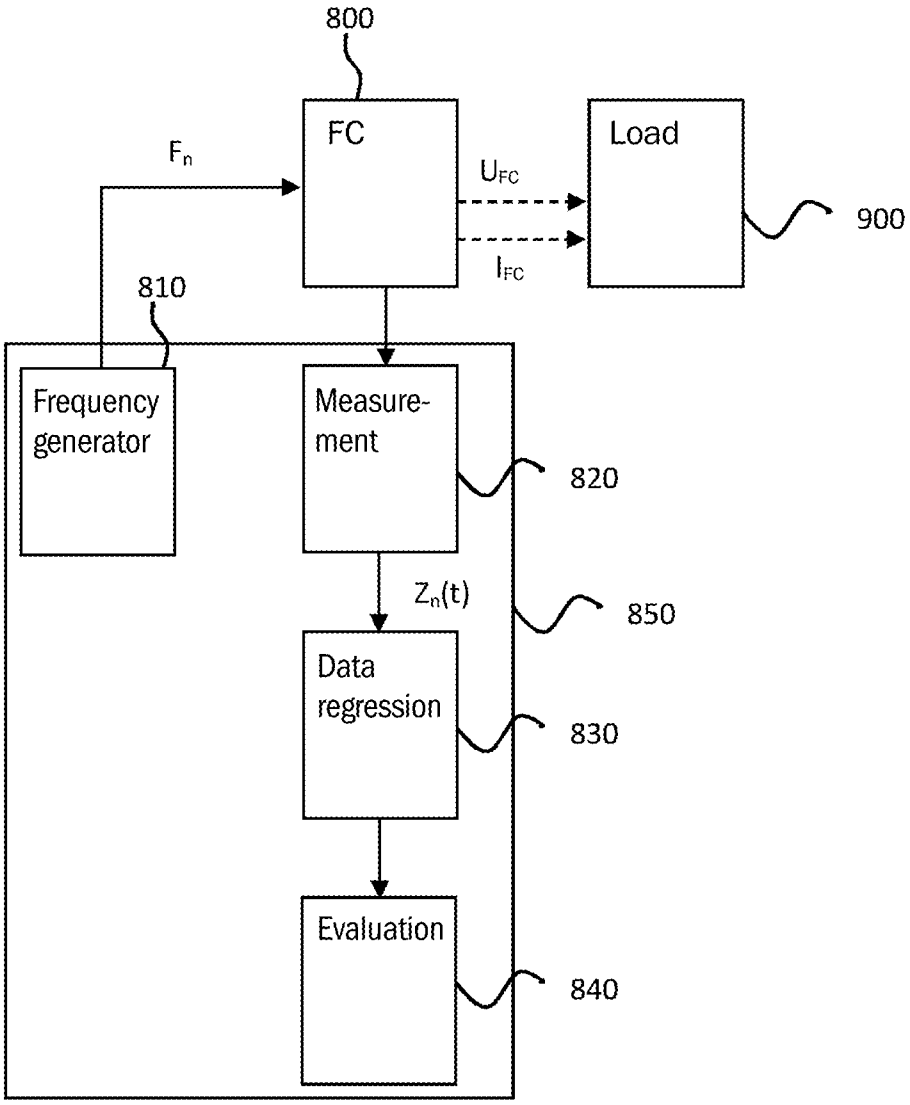
800
FC
Load
900
F_n
U_{FC}
I_{FC}
810
Frequency generator
Measure-ment
820
$Z_n(t)$
850
Data regression
830
Evaluation
840